Improved 2-norm-based Redundancy Resolution Methods

-With Application to Robotics-

２ノルムに基づく冗長性解消法性能向上の研究
— ロボット制御への適用 —

A Master Thesis Submitted to
The Department of Electrical Engineering
for the Degree of Master of Science

by

Travis Baratcart

Supervisor

Professor Takafumi Koseki

Department of Electrical Engineering
The University of Tokyo
August 2014

Contents

List of Figures

List of Tables

Abstract

Redundancy is a useful characteristic in a multitude of systems and is valued for its ability to endow dexterity and fault tolerance in systems operating in dynamic, remote, or unpredictable environments. Although useful, incorporation of redundancy in a system endows added complication in the control structure which needs to be resolved.

Easily the most popular method of resolving this redundancy is through application of the 2-norm optimizing pseudoinverse. Resolution through 2-norm optimization is very popularly utilized due to its analytical tractability: the 2-norm resolves systems uniquely, continuously, and often most importantly, in a very simple way. A well known problem exists in 2-norm resolution, however, in that it fails to make use of systems' full potential output space. Due to the complexity of alternatives, system designers tend to either ignore this problem and work within the bounds of 2-norm resolution or make use of methods to extend the resolution range of 2-norm resolution.

The most popular extension of the 2-norm is found in the Cascaded Generalized Inverse (CGI). CGI is an intuitive extension of 2-norm and prior to the work of this thesis held its place as the largest extension of 2-norm resolution.

In this work, three methods will be introduced based upon 2-norm resolution. The first two methods are modifications of CGI. It will be shown that although successful in extending the resolution range of 2-norm, CGI loses out on one of the main benefits of 2-norm resolution: continuity. Additionally, despite this drawback, CGI still does not attain the full output range of arbitrary systems.

The first proposed method, the Continuous Cascaded Generalized inverse (cCGI), is targeted at the first problem. cCGI is introduced as the largest extension of the 2-norm that ensures continuity of resolution. The continuity of CGI is analytically proven and the dynamic improvements when using cCGI, with respect to 2-norm and CGI, are simulated.

For systems in which this continuity is not a significant concern, or for such systems that have been sufficiently tested to ensure discontinuity does not arise, the Extended CGI (eCGI) is proposed. eCGI resolution is currently the largest extension of 2-norm resolution.

Both of these system are introduced and compared with application to kinematic redundancy in robotic manipulators.

Finally we look at a particular system, biarticular actuation redundancy, which is unique in that there exist multiple resolution schemes with the simplicity of 2-norm in implementation. The presence of these resolution solutions has allowed us to propose the first realization of 2-norm/Infinity-norm switching resolution. These two norms are physically preferable in opposite circumstances, and connecting the two allows for greater utility than either method used alone. The continuity of this switching system is analytically proven, and the system is experimentally implemented on a robot arm. It is shown that utilization of switching resolution improves both the motor size (with respect to 2-norm) and energy requirements (with respect to infinity-norm) of the system.

Acknowledgments

I never could have imagined I would have been made so welcome and make so many friends in my short time here.

First and foremost, I would like to thank Professor Koseki for his constant support and guidance. Without his belief and support the work of this thesis could never have come to fruition. His insights and criticisms have forced me to grow as a student, as a researcher, and as a person. He selflessly gave his time and never failed to put my needs above his.

Special thanks go out to Doctor Valerio Salvucci. I learned so much from him about academia, robotics, research. I selfishly occupied his time, and he never once complained. I can't even begin to imagine what my graduate experience would have been like if I hadn't had him as a constant jumping-off point.

Big thanks to Takada-san, Matsuzaki-san, and Ozaki-san. Their constant efforts allowed me to work, blissfully unaware of the immense university foundation supporting my study.

A great thank you to all the members of Koseki-lab. Your discussions have been a constant source of inspiration and welcome distraction. I'm so lucky to have been a part of your team. I will treasure your friendship forever.

Immense gratitude to those from the MEM and MEXT programs. Thanks to you I was lucky enough to focus entirely on my work without ever worrying for nourishment.

Thank you to the professors and staff of the Electrical Engineering Department. I've learned so much under your care.

Thank you to my family. Your support being so far from home has meant a lot. I never would have made it here without you.

Last but not least, thank you to Yvonne Teng. I can't even begin to list the many ways you've helped and supported me throughout these years. I never could have done this alone. Thank you so much.

Chapter 1

Introduction: Redundancy in Robotics

There is a growing trend of incorporating biologically-inspired elements in robotic systems. It rises from system designers' desire to, and the increasing practicality of, seeing their robotic platforms extend into the same environments we inhabit. Given human and animal ability to dexterously navigate even the most complex environments, it makes sense to consider some evolutionarily honed biological structures for their utility. As it turns out, many of the ways in which biology deviates from conventional robotics approaches have to do with the redundancy of these systems.

Three main types of redundancy have been adapted from biological systems to be used in improving robot manipulation: kinematic redundancy, manipulator redundancy, and actuation redundancy.

1.1 Kinematic redundancy

The most popularly utilized type of redundant system in robotics, kinematic redundancy involves additional degrees of motion than are necessary to accomplish the task. Consider a planar manipulator operating in 2-dimensional space. Such motion can be achieved by a manipulator with only two links and two joints (three, if orientation is also a restriction). Our arms are not so simple though. Operating in 3-dimensional space, there exist three position variables and three orientation variables to be realized by our arms. However, our arms are modeled as a 7 degree-of-freedom (DoF) manipulator as seen in Fig. 1.1 [1].

Incorporation of kinematic redundancy in robotics and our own arms endows numerous advantages in control. Kinematic redundancy adds a degree of decoupling of the individual joint coordinates and the end-effector coordinates. The

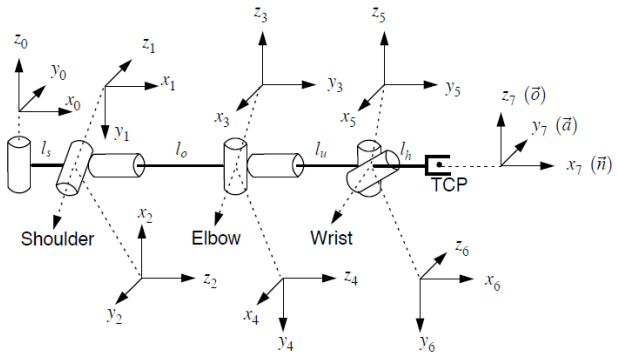

Figure 1.1: Kinematic model of human arm [1]

first and largest benefit of this is that it allows for object avoidance behavior due to the numerous potential joint configurations realizing the same end-effector position [2].This characteristic also extends the range of manipulation of our arms. Each of our joints have certain physical limits (the elbow being an obvious example). The added degrees of motion in our arms enable us to re-task motion to other more suitable joints if one joint reaches its limits of motion [3]. Such re-tasking can also be conducted in the event an actuator fails. This may lead to an elimination of redundancy in the arm, but still maintains the capability to realize the desired task. Finally, these added degrees-of-freedom enable motion and force output optimized by some physical quantities. For instance, when pushing a heavy load a human naturally does so in a way to maximize their leverage. If there were only one possible joint configuration to contact the load, this would not be possible. Each of these control options have obvious advantages applied to robotic manipulators.

Arguably the truest realization of such human bio-mimicry is found in the DLR arm [4], seen in Fig. 1.2. Functionally identical to a human arm, the DLR arm has 3 degrees of freedom in the shoulder, 1 in the elbow, 2 in the forearm, and 19 in the hand. The structure of the DLR arm makes it suitable in human motion capture, study of human biomechanics, and development of humanoid robots.

Kinematic redundancy can also be use to surpass the dexterous capabilities of humans. This aim is seen in hyper-redundant manipulators. Hyper-redundant manipulators have far more degrees of freedom than are necessary for the desired task. One such hyper-redundant manipulator is the Insertable Robotic Effectors Platform (IREP) [5] as seen in Fig. 1.3. The IREP system is composed of two 9-DoF arms and is aimed at the application of minimally invasive surgery. The IREP system successfully realizes single-port entry surgery, which has the capability to drastically improve patient care, but is impossible given human levels of dexterity.

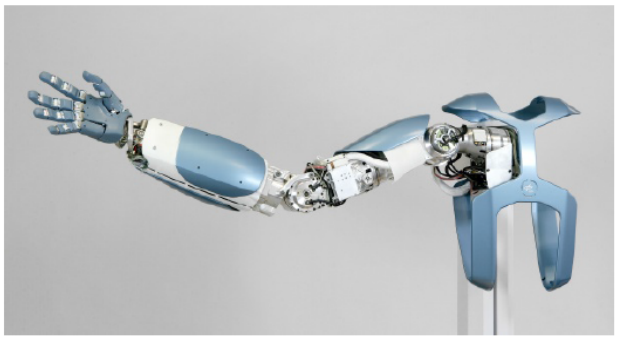

Figure 1.2: DLR hand-arm system [4]

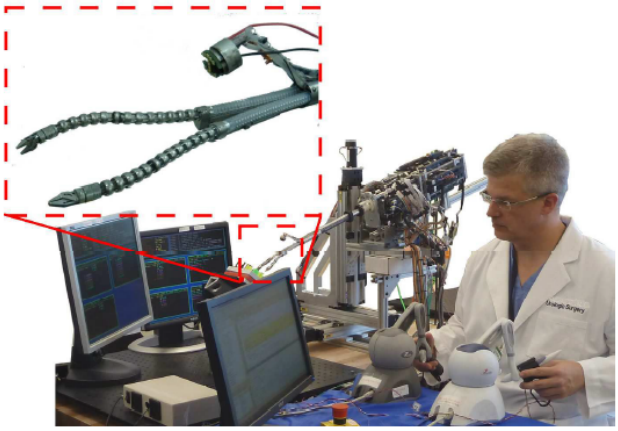

Figure 1.3: IREP hyper-redundant surgery system [5]

Utilizing the IREP system allows the surgeon to dexterously guide the path of the end-effector using a controller from outside the patient's body.

1.2 Manipulator redundancy

The second major type of redundancy in robotics is that of manipulator redundancy. Single, serial-manipulators (like the human arm) have numerous advantages. They have large workspaces, are cheaply and easily implemented, and are simple to control. However humans, for good reason, do not always use their limbs in serial configurations. Serial manipulators cannot lift large loads and are difficult to precisely control when loaded[6].

When precision or strength are required, we tend to use our limbs in parallel.

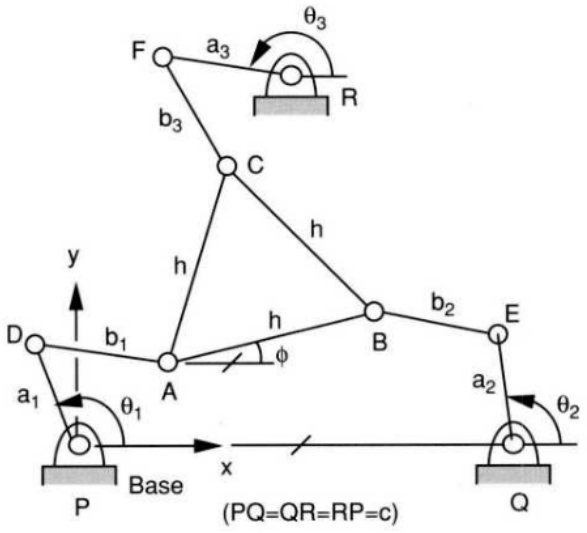

Figure 1.4: Example system with manipulator redundancy used in discussion [7]

We of course use both arms when we lift heavy loads. We also use three fingers in parallel to realize the precise movements necessary for writing.

To understand the physical justification for this, consider the example parallel manipulator structure [7] in Fig. 1.4. The platform has three, 2-DoF manipulators actuating it in 2-dimensional space. Therefore there exist three degrees-of-freedom (two position, one orientation) to be actuated by these six joints acting upon it.

If this platform were to be actuated by a single, serial manipulator, it would need to be a 3-link manipulator. Additionally it would need to be far longer in order to be able to realize the same workspace. Being simultaneously manipulated by three manipulators then reduces the distance from the base in which a load or disturbance force is applied. This reduces the torques applied at each joint and results in overall increased stiffness of the system. If compliant elements are used in the joints, this reduces the displacement of the arm in response to load or disturbance. If the joints are not compliant this increases the force the manipulator can withstand before it bends or breaks. Additionally, such systems are usually designed so that the stiffnesses of each manipulator compensate each other, i.e. one manipulator should always be able to resist disturbance for the benefit of the whole system.

Manipulator redundancy has therefore found its place early in industrial applications, lifting heavy loads and performing precise manipulations [8, 9, 10].

1.3 Actuator redundancy

The final type of redundancy influencing robotic manipulators is that of actuation redundancy. Conventional robotics states that for each joint to be actuated, one motor should be supplied to provide the necessary torque. While straightforward, this is not how our bodies work. There are over 20 muscles actuating the seven degrees-of-freedom in our arms [11]. Part of the reason for this high level of redundancy is due to the difficulty of a biological actuator to produce force in two directions. Our muscles are only capable of pulling, so they come in pairs to provide force in each direction. But this only accounts for 14 muscles to actuate seven degrees-of-freedom. Pairs of muscles, called biarticular muscles, also exist which provide torque about multiple joints simultaneously.

It turns out there are a multitude of advantages in the complicated actuation structure of our arms. The first arises from the unique physical characteristics of our muscles. Unlike the linear springs we are used to dealing with, the tension in our muscles is nonlinear with respect to displacement as seen in the muscle model [12] in Fig. 1.5. This allows for simultaneous regulation of force and stiffness through co-contraction. The advantage of stiffness regulation has already found its consumer application in variable series elastic actuators (VSA's) [13]. VSA's, similar to our own muscles, are actuators with two motors which are capable of simultaneously controlling output torque and stiffness. These actuators are very useful in robotic systems intended to work with humans, as compliance is fundamental to safety in robotics. The previously discussed DLR arm [4] makes use of VSA's in its joints to ensure the safety of the surrounding individuals a humanoid robot would no doubt interact with.

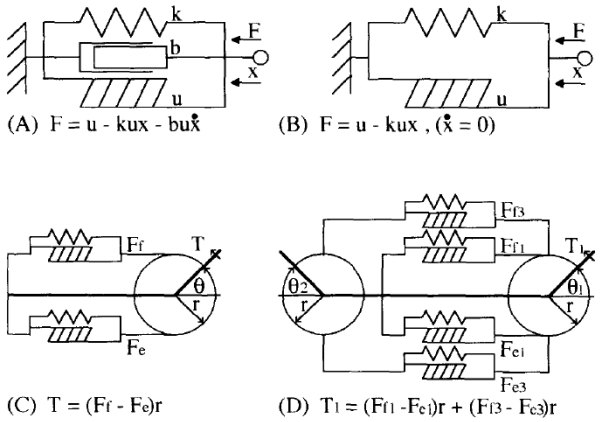

Figure 1.5: Model of human muscle, leading to stiffness modulation [12]

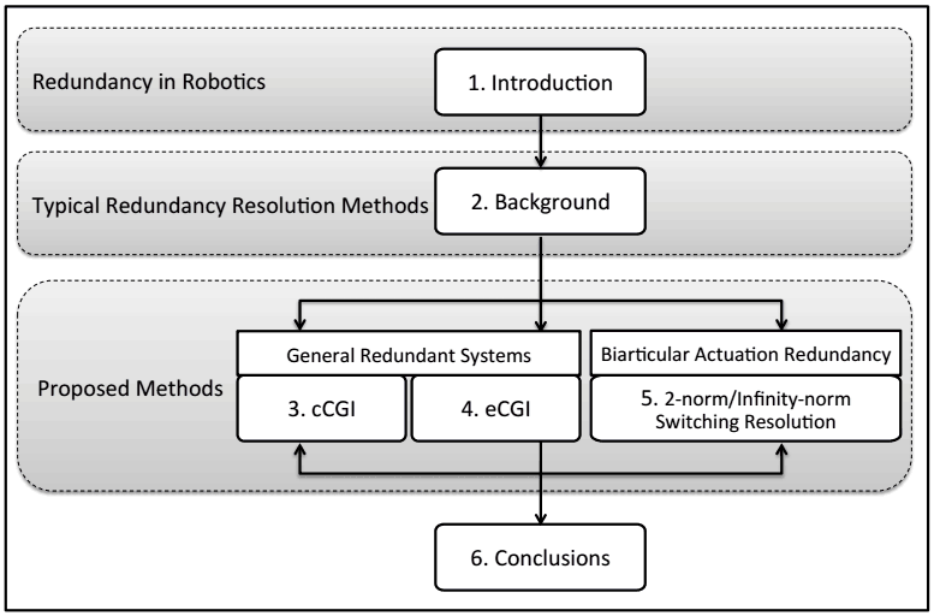

Figure 1.6: Thesis Structure

Biarticular actuation additionally allows for several useful control characteristics. Activation of biarticular muscles allows for force transfer from proximal to distal joints [14], allowing for a reduction in limb inertia by moving stronger muscles toward the core. Due to the geometry of biarticular actuation, it additionally improves output force [15] and stiffness homogeneity [C6, C7]. Biarticular actuation is currently a popular topic of research in mechatronics, being applied to realize some of these same useful characteristic [16, 17, 18, 19, 20].

1.4 Thesis structure

The structure of this thesis is outlined in Fig. 1.6

In Chapter 2, the mathematical formulation of redundancy as well as some related resolution techniques will be introduced. Chapters 3-5 are the contribution of this thesis. Chapter 3 introduces the Continuous Cascaded Generalized Inverse (cCGI) which is the largest extension of 2-norm for systems that demand continuity. Chapter 4 introduces the the Extended Cascaded Generalized Inverse (eCGI) which is the largest extension of 2-norm, but without the guarantee of continuity in resolution. Finally, Chapter 5 introduces 2-norm/Infinity-norm Switching Resolution of biarticular actuation redundancy. Conclusions are given in Chapter 6.

Chapter 2

Background

This problem of redundancy is considered as follows: The matrix $\boldsymbol{B} \in \Re^{mxn}$ translates input variables $\boldsymbol{u} \in \Re^n$ to output values $\boldsymbol{v} \in \Re^m$ as follows:

$$\boldsymbol{v} = \boldsymbol{B}\boldsymbol{u} \tag{2.1}$$

If $n = m$ the system is said to be deterministic, and if $\boldsymbol{B}$ is nonsingular, a unique selection of inputs $\boldsymbol{u}$ can be selected to realize a desired output $\boldsymbol{v}$. If $n > m$ the system is said to be redundant, and if in a non-singular configuration, there exist an infinite number of input selections to realize a desired output.

2.1 2-norm resolution

By far the most popular method of resolving this redundancy is through optimization of the 2-norm of resolved inputs [21], or

$$\min\left(\sqrt{u_1^2 + u_2^2 + ... + u_n^2}\right) \tag{2.2}$$

2-norm optimization can be accomplished through utilization of the Moore-Penrose pseudoinverse [22] which resolves the system redundancy as

$$\boldsymbol{u} = \boldsymbol{B}^{\dagger}\boldsymbol{v} \tag{2.3}$$

where if $\boldsymbol{B}$ is full row rank, the pseudoinverse, $\boldsymbol{B}^{\dagger}$, of $\boldsymbol{B}$ is defined as:

$$\boldsymbol{B}^{\dagger} := \boldsymbol{B}^T(\boldsymbol{B}\boldsymbol{B}^T)^{-1} \tag{2.4}$$

Resolution using the 2-norm is by far the most popular method due to it's analytical tractability: it resolves systems uniquely, continuously, and foremost in a simple closed-form solution. Physically, as a minimization of a sum of squares, an

analog can be drawn between 2-norm optimization and an optimization of energy or power [23]. Resolution using the two-norm does have a well-known drawback however in its failure to exploit a system's full output space if input bounds are imposed.

The reason for this is simply that a 2-norm optimal input resolution does not necessarily yield a result within arbitrary input bounds. This often leads to 2-norm yielding unfeasible resolutions despite the existence of feasible alternatives.

2.2 Infinity-norm resolution

Recognizing this problem, many researchers have put forth alternative resolution schemes which do not suffer from this drawback. One such popular method is resolution using the infinity-norm [24, 25, 26, 27], or

$$\min\left(\max\left(\left|u_1\right|,\left|u_2\right|,...,\left|u_n\right|\right)\right) \tag{2.5}$$

subject to the task constraint, (2.1).

Minimization of infinity-norm is equivalent to a minimum-effort solution, as it will only allow for a maximum system-wide exertion if it is absolutely necessary considering the task output. Infinity-norm resolution suffers in application however due to its more complicated implementation — infinity-norm optimization usually involves application of a numerical algorithm to locate an infinity-norm optimal solution. Issues of continuity also exist in infinity-norm optimization arising from occasional lack of uniqueness of an infinity-norm optimal solution [28].

Issues such as these in infinity-norm resolution and other resolution methods in competition with 2-norm have led to the majority of implementations to continue using 2-norm and abandoning the lost output space.

2.3 Extending the resolution range of the 2-norm

For applications in which this lost output space is a serious concern, system designers tend not to switch resolution approaches entirely. Rather, methods to extend the output range of the 2-norm are typically utilized.

2.3.1 Least-Squares with Clipping

By far the simplest approach to extending the resolution range of 2-norm is Least-Squares with Clipping [29]. As the name implies, Least-Squares with Clipping involves simple application of the Moore-Penrose Pseudoinverse as seen in (2.3)

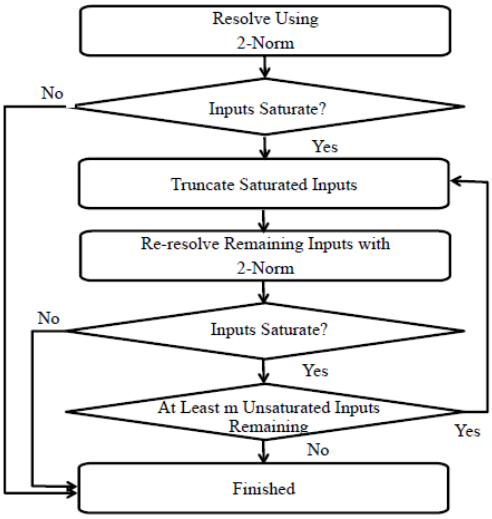

Figure 2.1: Flowchart of Cascaded Generalized Inverse redundancy resolution.

and (2.4) and truncating any inputs resolved in excess of their input bounds. Although simple, Least-Squares with Clipping will fail to realize the desired output whenever 2-norm fails resolution. Consequently, most system designers prefer more sophisticated approaches in extending the resolution range of the 2-norm.

2.3.2 The Redistributed Pseudoinverse

The Redistributed Pseudoinverse is a first step at actually extending the resolution range of the 2-norm [30]. The process is described as follows:

1. Find the pseudoinverse resolution of the system. If all resolved inputs lie within their output bounds, the process ends.

2. If any resolved inputs lie outside their output bounds, the corresponding inputs are truncated to the respective maximums or minimums.

   The new system created, corresponding to the un-maximized inputs and the desired output minus the contributions of the maximized inputs, is then resolved using the pseudoinverse.

The Redistributed Pseudoinverse does indeed extend the resolution range of the 2-norm for a period. However, as the process of re-resolution is carried out again using 2-norm, the re-resolution will suffer from the same failings as the 2-norm: the output range of the re-resolution is not fully exploited.

2.3.3 The Cascaded Generalized Inverse (CGI)

The Cascaded Generalized Inverse (CGI) [31] is the above problem in re-resolution. Whereas the Redistributed Pseduoinverse only re-resolves the system once, CGI repeats the process indefinitely if the re-resolutions are also unfeasible, as seen in block diagram of the method in Fig. 2.1. CGI was, prior to the work outlined in this thesis, the largest and most popularly utilized extension of 2-norm resolution.

Variations exist where the process continues until the resultant system is represented by an invertible square matrix, one variable is arbitrarily saturated in each iteration in the interest of speed [32], and the ”most” saturated variable is saturated each iteration to preserve directionality at the expense of speed [33]. The Cascaded Generalized Inverse has been applied to many problems including aircraft control allocations [34, 35], VTOL control systems [36], ship berthing [37], and ship positioning systems [38].

Chapter 3

Continuous Cascaded Generalized Inverse Resolution (cCGI)

In this chapter it will be shown that although successful in extending the resolution range of 2-norm, CGI loses out on one of the main benefits of 2-norm resolution: continuity. A proposed alternative, Continuous Cascaded Generalized Inverse (cCGI) approach to redundancy resolution will be introduced and some dynamic benefits when applied to kinematic redundancy demonstrated. Sections 3.1 and 3.2 are the work of [C2]. Section 3.3 is the work of [C4]

3.1 Discontinuity in CGI

In this section we will demonstrate the issue of discontinuity in CGI through consideration of an example resolution implementation. The considered system is the four-link kinematically-redundant planar manipulator. The problem of kinematic-redundancy is a particular example of (2.1) and is formulated as follows. The manipulator Jacobian, $\boldsymbol{J}$, relates joint velocities, $\dot{\boldsymbol{q}}$, to end-effector velocity, $\boldsymbol{v}_{\text{eff}}$ as follows:

$$\boldsymbol{v}_{\text{eff}} = \boldsymbol{J}\dot{\boldsymbol{q}} \tag{3.1}$$

where

$$[\boldsymbol{J}]_{(i,j)} = \frac{\delta[x_{\text{eff}}]_i}{\delta q_j} \tag{3.2}$$

In our case of a 4 link manipulator, there exist four joint space inputs to the 2-dimensional end-effector output, so there are two degrees of redundancy in this system to be resolved.

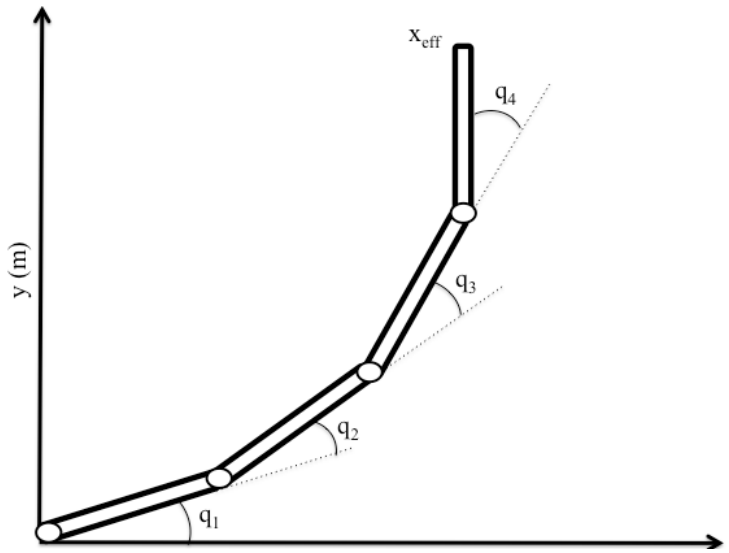

Figure 3.1: 4-link planar manipulator used for demonstration of discontinuity in CGI Resolution

Consider a 4-link manipulator, as shown in Fig. 3.1, in Configuration A which will be defined as the following:

Configuration A :=

$L_1 = L_2 = L_3 = L_4 = 1$ (unit)

$\boldsymbol{q} = [\frac{\pi}{32}, \frac{\pi}{6}, \frac{\pi}{6}, \frac{\pi}{6}]$ (rad)

$\dot{\boldsymbol{q}}_{\max} = [1, 2, 10, 10]$ (rad/sec)

Fig. 3.2 illustrates the resolved joint velocities necessary to produce a given end-effector velocity in the direction $\theta = 0$. The results of redundancy resolution are shown carried out by both 2-norm resolution and CGI.

It is seen that when the 2-norm resolution of $\dot{q}_2$ exceeds the maximum limit, at $\|\mathbf{v}\| \approx 11$ units/sec, the discrepancy between this resolution and second-level resolution associated with maximized $\dot{q}_1$ causes a discontinuity affecting joints q_2, q_3, and q_4.

Such discontinuity is often impossible to realize in the resolved system. In our example, using CGI demands discontinuous changes in joint velocity, which is clearly impossible. Attempting to realize the CGI resolution may lead to undesirable dynamic effects as well as instability. It is desirable in many applications then to find an extension of the 2-norm that would not lead to such discontinuity in resolution. Our answer to that is the Continuous Cascaded Generalized Inverse (cCGI).

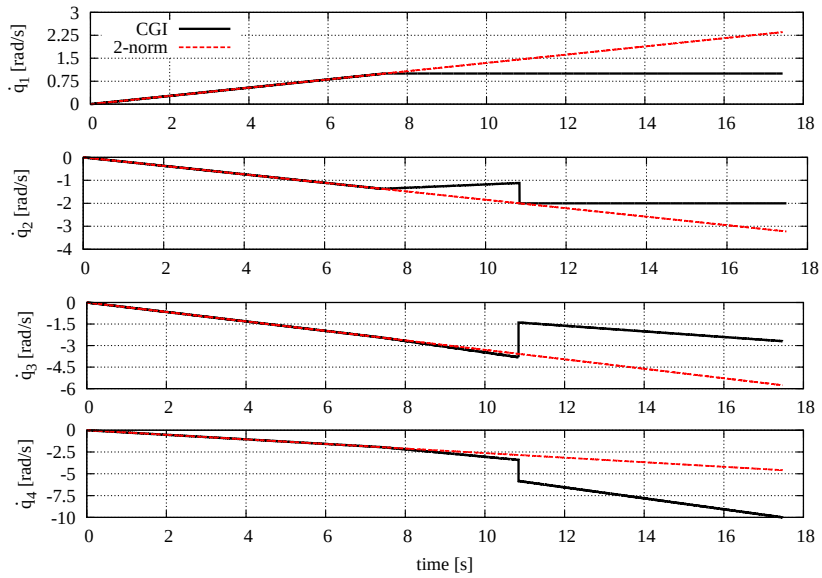

Figure 3.2: Static resolution of kinematic redundancy using CGI. CGI continues resolution by discontinuously reassigning velocity amongst q_2, q_3, and q_4.

3.2 Proposal: Continuous Cascaded Generalized Inverse Resolution (cCGI)

We note that discontinuity in CGI is triggered by discrepancy between different levels of pseudoinverse resolution and re-resolution. With that in mind, it seems reasonable then that restricting CGI such that only one input may saturate per resolution level will eliminate risk of discontinuity. For this proposed system, consider the initial pseudoinverse resolution as one level, and each subsequent process of truncation and re-resolution as another level. This process was deemed the Continuous Cascaded Generalized Inverse or cCGI. Although most intuitively implemented recursively as in Fig. 2.1 (with the added domain restriction), cCGI can also be represented in the following closed-form expression.

Define $\boldsymbol{B}_i$ as the i'th column of $\boldsymbol{B}$ and $\boldsymbol{B}'_{i_1.i_2...i_z}$ as the matrix $\boldsymbol{B}$ with the i_1, i_2, ... , and i_z'th column removed. Likewise define u_i as the i'th element of $\boldsymbol{u}$, and $\boldsymbol{u}'_{i_1.i_2...i_z}$ as the vector $\boldsymbol{u}$ with the i_1, i_2, ... , and i_z'th element removed.

Parentheticals are used following input values to denote the resolution of the inputs in the corresponding case. For example, $u_3(1(\text{a}))$ and $\boldsymbol{u}'_3(1(\text{a}))$ refer respectively to the values of the third element of $\boldsymbol{u}$ and the vector $\boldsymbol{u}$ with the third element removed attained in the case 1(a). If inputs are referred to without parentheticals, it will refer to the value attained from the currently discussed case.

Case 0 :

$$\boldsymbol{u} = \boldsymbol{B}^{\dagger}\boldsymbol{v} \tag{3.3}$$

Case $i_1(\mathrm{a})$:

$$u_{i_1} = u_{i_1}^{\max} \tag{3.4}$$

$$\boldsymbol{u}'_{i_1} = (\boldsymbol{B}'_{i_1})^{\dagger}(\boldsymbol{v} - \boldsymbol{B}_{i_1} u_{i_1}^{\max}) \tag{3.5}$$

Case $i_1(\mathrm{b})$

$$u_{i_1} = -u_{i_1}^{\max} \tag{3.6}$$

$$\boldsymbol{u}'_{i_1} = (\boldsymbol{B}'_{i_1})^{\dagger}(\boldsymbol{v} + \boldsymbol{B}_{i_1} u_{i_1}^{\max}) \tag{3.7}$$

Case $i_1(x_1).i_2(x_2)...i_{z-1}(x_{z-1}).i_z(\mathrm{a})$:

$$u_{i_1} = \begin{cases} u_{i_1}^{\max} & \text{if } x_1 = \mathrm{a} \\ -u_{i_1}^{\max} & \text{if } x_1 = \mathrm{b} \end{cases} \tag{3.8}$$

$$\vdots$$

$$u_{i_{z-1}} = \begin{cases} u_{i_{z-1}}^{\max} & \text{if } x_{z-1} = \mathrm{a} \\ -u_{i_{z-1}}^{\max} & \text{if } x_{z-1} = \mathrm{b} \end{cases} \tag{3.9}$$

$$u_{i_z} = u_{i_z}^{\max} \tag{3.10}$$

$$\boldsymbol{u}'_{i_1 \ldots i_z} = (\boldsymbol{B}'_{i_1 \ldots i_z})^{\dagger}(\boldsymbol{v} - \sum_{\gamma=1}^{z} \boldsymbol{B}_{i_\gamma} u_{i_\gamma}) \tag{3.11}$$

Case $i_1(x_1).i_2(x_2)...i_{z-1}(x_{z-1}).i_z(\mathrm{b})$:

$$u_{i_1} = \begin{cases} u_{i_1}^{\max} & \text{if } x_1 = \mathrm{a} \\ -u_{i_1}^{\max} & \text{if } x_1 = \mathrm{b} \end{cases} \tag{3.12}$$

$$\vdots$$

$$u_{i_{z-1}} = \begin{cases} u_{i_{z-1}}^{\max} & \text{if } x_{z-1} = \mathrm{a} \\ -u_{i_{z-1}}^{\max} & \text{if } x_{z-1} = \mathrm{b} \end{cases} \tag{3.13}$$

$$u_{i_z} = -u_{i_z}^{\max} \tag{3.14}$$

$$\boldsymbol{u}'_{i_1 \ldots i_z} = (\boldsymbol{B}'_{i_1 \ldots i_z})^{\dagger}(\boldsymbol{v} - \sum_{\gamma=1}^{z} \boldsymbol{B}_{i_\gamma} u_{i_\gamma}) \tag{3.15}$$

and define

$$\text{case } 0 := |u_i(0)| \leq u_i^{\max}, \forall i \in [1,n] \tag{3.16}$$

$$\text{case i(a)} := u_i(0) > u_i^{\max}, |u_j(0)| \leq u_j^{\max}, \forall j \neq i \tag{3.17}$$

$$\text{case i(b)} := u_i(0) < -u_i^{\max}, |u_j(0)| \leq u_j^{\max}, \forall j \neq i \tag{3.18}$$

$$\begin{aligned}&\text{Case } i_1(x_1).i_2(x_2)...i_{z-1}(x_{z-1}).i_z(\text{a}) := \\ &\quad (\text{Case } i_1(x_1).i_2(x_2)...i_{z-1}(x_{z-1})), \\ &\quad (u_{i_z}(i_1(x_1).i_2(x_2)...i_{z-1}(x_{z-1})) > u_{i_z}^{\max}), \\ &\quad \text{and } (|u_{i_j}(i_1(x_1).i_2(x_2)...i_{z-1}(x_{z-1}))| \leq u_{i_j}^{\max}, \forall j \neq z)\end{aligned} \tag{3.19}$$

$$\begin{aligned}&\text{Case } i_1(x_1).i_2(x_2)...i_{z-1}(x_{z-1}).i_z(\text{b}) := \\ &\quad (\text{Case } i_1(x_1).i_2(x_2)...i_{z-1}(x_{z-1})), \\ &\quad (u_{i_z}(i_1(x_1).i_2(x_2)...i_{z-1}(x_{z-1})) < -u_{i_z}^{\max}), \\ &\quad \text{and } (|u_{i_j}(i_1(x_1).i_2(x_2)...i_{z-1}(x_{z-1}))| \leq u_{i_j}^{\max}, \forall j \neq z)\end{aligned} \tag{3.20}$$

The continuity of cCGI is analytically proven in Appendix A.

3.3 Dynamic analysis

3.3.1 Setup

In the following section the dynamic effects of the discontinuity in CGI, in addition to how they are alleviated applying cCGI will be analyzed.

We will consider another 4-link kinematically redundant manipulator, similar to the one utilized in Sec. 3.1. For ease of understanding of calculations, the manipulator was selected as having 1 kg, 1 m links and link inertia values perpendicular to the direction of rotation, I_{z_i}, were all set at unit value. Maximum joint velocities were set as $\dot{\boldsymbol{q}}^{\max} = [0.5, 0.7, 5.0, 5.0]$ (rad/sec). The manipulator is assumed to be planar, so gravity terms can be neglected.

Additionally, we choose to model the joint stiffness. This stiffness is typically assumed to be infinite to simplify calculation, but it will nevertheless affect the dynamic performance of the arm. Considering the large torque and jerk which will be applied as a result of the discontinuously resolved velocities, it seems likely that this finite joint stiffness will play a role. The dynamics of such a manipulator can be described by the following expression:

$$\boldsymbol{M}(\boldsymbol{q})\ddot{\boldsymbol{q}}+\boldsymbol{C}(\boldsymbol{q},\dot{\boldsymbol{q}})+\boldsymbol{g}(\boldsymbol{q})+\mathbf{D}(\dot{\boldsymbol{q}}-\dot{\boldsymbol{\theta}})+\mathbf{K}(\boldsymbol{q}-\boldsymbol{\theta})=0 \tag{3.21}$$

$$\boldsymbol{M}_j\ddot{\boldsymbol{\theta}}+\mathbf{D}(\dot{\boldsymbol{\theta}}-\dot{\boldsymbol{q}})+\mathbf{K}(\boldsymbol{\theta}-\boldsymbol{q})=\boldsymbol{\tau} \tag{3.22}$$

where $\boldsymbol{M}\in\Re^{nxn}$ is the manipulator inertia matrix, $\boldsymbol{M}_j\in\Re^{nxn}$ is the diagonal motor inertia matrix, $\boldsymbol{C}\in\Re^{nx1}$ is the vector of Coriolis and centrifugal force terms, $\boldsymbol{g}\in\Re^{nx1}$ is the vector of gravity terms, $\boldsymbol{\tau}\in\Re^{nx1}$ is the applied joint torque, $\mathbf{K}\in\Re^{nxn}$, $\boldsymbol{\theta}\in\Re^{nx1}$ are the motor coordinates, and $\mathbf{D}\in\Re^{nxn}$ are the diagonal matrices of joint stiffness and joint damping terms, respectively [39].

Joint stiffness values are chosen as $\mathbf{K}=100000\boldsymbol{I}_4$ (N/rad), which is chosen as approximately 1 order of magnitude above common high stiffness threshold of variable series elastic motors. Joint damping should be considered nonzero, but much less than joint stiffness, so values of $10\boldsymbol{I}_4$ (N·s/rad) were chosen.

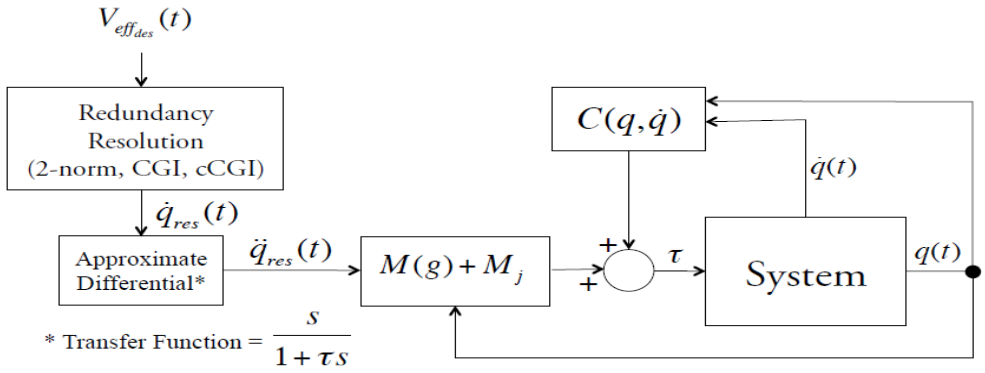

Figure 3.3: Block diagram describing open-loop control of kinematically redundant planar arm

The block diagram of the control structure utilized is seen in 3.3. In order to effectively isolate the effect of the discontinuity, an open-loop control is used. In the dynamic compensation, the joint stiffnesses are assumed to be infinite, as this is a typical approach. However in the plant model, the finite joint stiffness is considered. This allows for observation of the unexpected results of finite stiffness while using a standard compensation model which neglects these terms.

In the dynamic analysis we neglect friction, as the effect is equivalent to damping in the region of interest. Backlash is neglected as both motors and gears without backlash exist. Time delay is neglected as open loop control is utilized and the physical system is time-invariant.

The described arm is commanded from rest at an initial position $\boldsymbol{q}=\boldsymbol{\theta}=[0,\frac{\pi}{4},\frac{\pi}{4},\frac{\pi}{3}]$ (rad) to move with a straight-line end-effector trajectory 1 m in the direction $\phi=\frac{\pi}{4}$ (rad) with a velocity trajectory as described in Fig. 3.4 and resolved

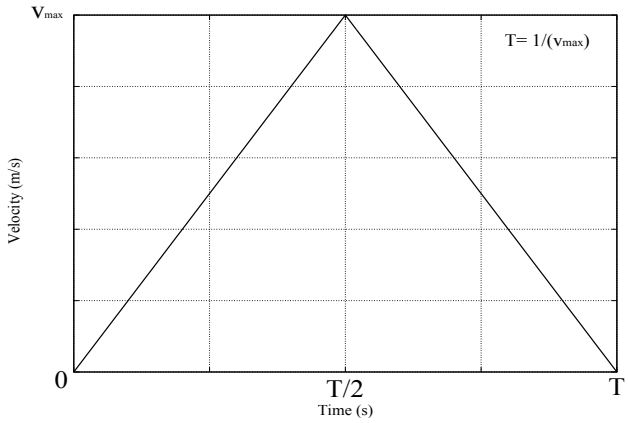

Figure 3.4: Velocity profile used in demonstrating effects of discontinuity. The arm is commanded to travel 1 m with a given maximum velocity.

using CGI resolution for arbitrary $v_{\max}$. The system updates with a frequency of $\frac{1}{\Delta T} = 10$ kHz, and τ for the differential calculation is selected as 10 ms.

The structure of the velocity waveform allows variation of $v_{\max}$ to take CGI through its three levels of resolution: CGI equivalent to both 2-norm and cCGI resolution; CGI equivalent to cCGI resolution; and exclusively CGI resolution

3.3.2 Results

Figure 3.5 illustrates the simulation conducted with $\mathrm{v}_{\max}$ set sufficiently low that CGI resolution is equivalent to 2-norm resolution. For this simulation, $\mathrm{v}_{\max}$ is set as 2.5 m/sec which is very close to the failure region of 2-norm. It is seen that the actual trajectory follows the intended trajectory fairly precisely. Some small oscillation is introduced by the discontinuous torque applied at the midway point, but that is quickly suppressed by system damping. Slight delay is also seen as due to the approximate differential utilized in the control scheme, but this occurs regardless of resolution method.

Figure 3.6 illustrates the simulation conducted with $\mathrm{v}_{\max}$ set sufficiently high that, of the three considered methods, only CGI can resolve the system. That is to say, 2-norm yields unrealizable results, and the CGI resultant violates the conditions of cCGI resolution. Simulation is conducted with a maximum velocity of $\mathrm{v}_{\max} = 5$ (m/sec). At $t \approx 0.085$ s, a discrepancy occurs between the saturated value of $\dot{q}_2$ in the 2-norm resolution and the re-optimization against saturated $\dot{q}_1$. This causes CGI to discontinuously redistribute velocity contributions amongst $\dot{q}_2$, $\dot{q}_3$, and $\dot{q}_4$. This discontinuity in the resolved velocity yields large acceleration and jerk, even despite the approximate differential. This causes large joint veloc-

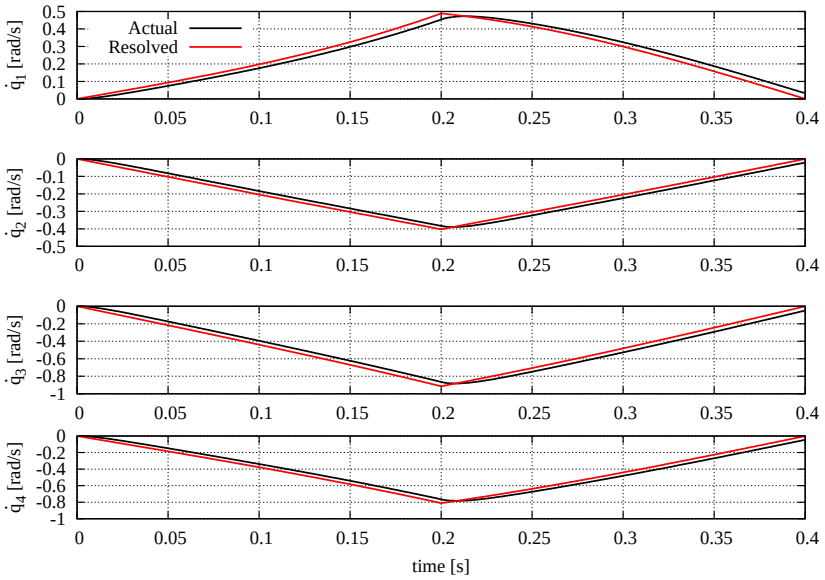

Figure 3.5: Joint velocities of trajectory realizable with pseudoinverse Redundancy Resolution

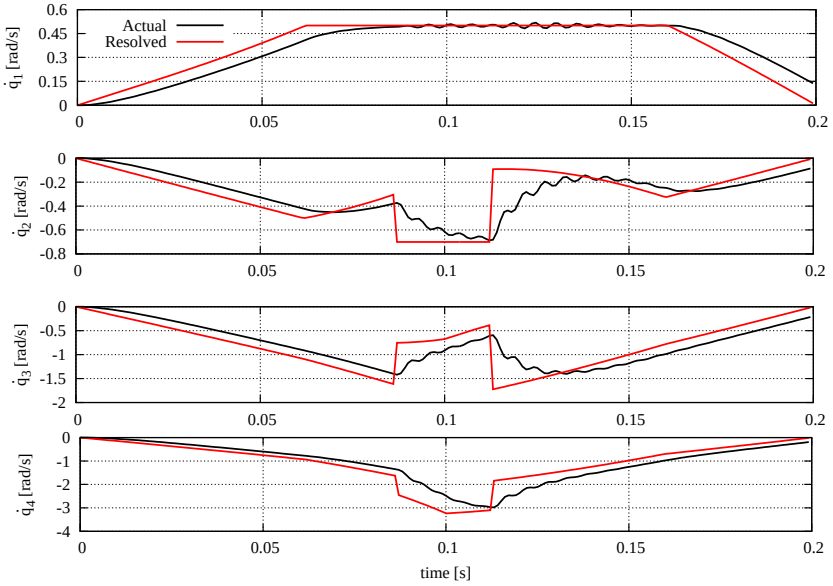

Figure 3.6: Joint velocities of trajectory realizable only with CGI resolution. Discontinuously resolved velocities generate velocity oscillation and error.

ity oscillation and error, which is exacerbated upon deceleration when the same happens again.

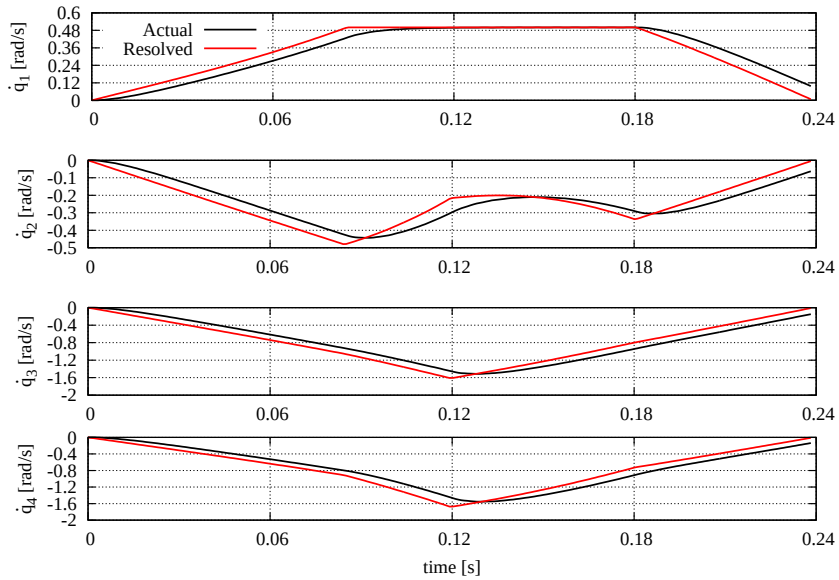

Figure 3.7: Joint velocities of trajectory unrealizable with 2-norm, but realizable with Continuous CGI resolution. Resolution is guaranteed continuous, so the large oscillation observed in standard CGI resolution is not observed.

Figure 3.7 illustrates the simulation repeated with v_{max} set such that CGI is equivalent to cCGI resolution. For this simulation maximum velocity, v_{max} is set as 4.2 (m/sec). As anticipated the resultant resolved velocities are continuous. This results in a realized velocity trajectory with similar dynamic properties to 2-norm but with only a 19 percent increase in time over the previously considered example (still a large improvement over 2-norm).

Figure 3.8 illustrates the maximum velocity error observed with CGI resolution for the given maximum velocity, or

$$\max(|\dot{q}_i(t) - \dot{q}_i^{\text{res}}(t)|) \tag{3.23}$$

where $\dot{q}_i^{\text{res}}$ is the resolved solution for $\dot{q}_i$.

As our examples have shown, error remains low and increases at a fairly constant rate throughout the 2-norm and cCGI equivalence region. However, as soon as cCGI fails resolution, the discontinuity which occurs in CGI resolution creates sudden large error.

Fig. 3.9 illustrates the maximum achievable velocities (scaled down by a factor of 10) in all directions in configuration A, using 2-norm, CGI, and constrained

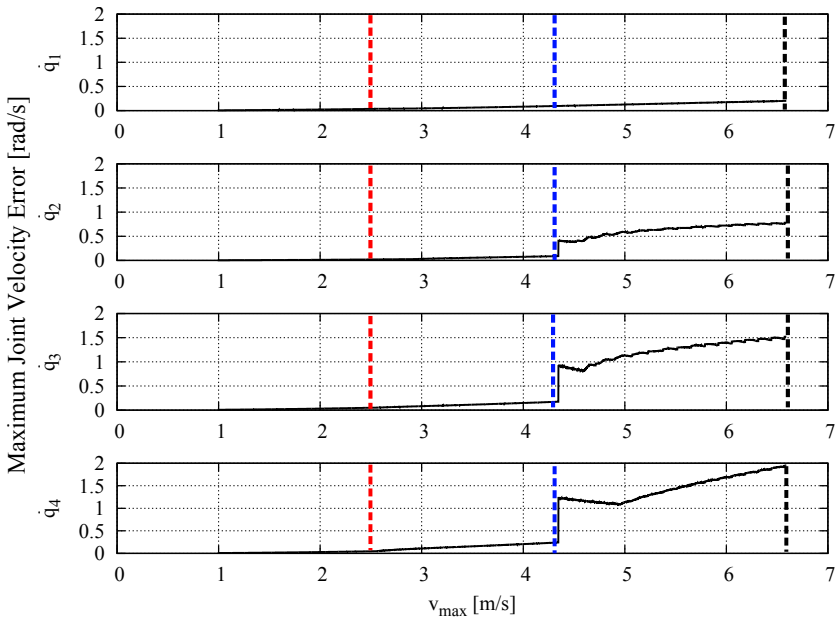

Figure 3.8: Maximum joint velocity error given maximum end-effector velocity. 2-norm, cCGI, and CGI stop resolving the system at the red, blue, and black dotted-lines, respectively. Magnitude remains low through 2-norm and cCGI resolution, but rapidly increases once cCGI stops resolution.

CGI. It is seen that while always greater than or equal to that achieved with 2-norm, the maximum velocity of constrained CGI is always less than or equal to unconstrained CGI. As such, for applications in which the effects of discontinuities in resolution are not an issue, it would be preferable to still use unconstrained CGI.

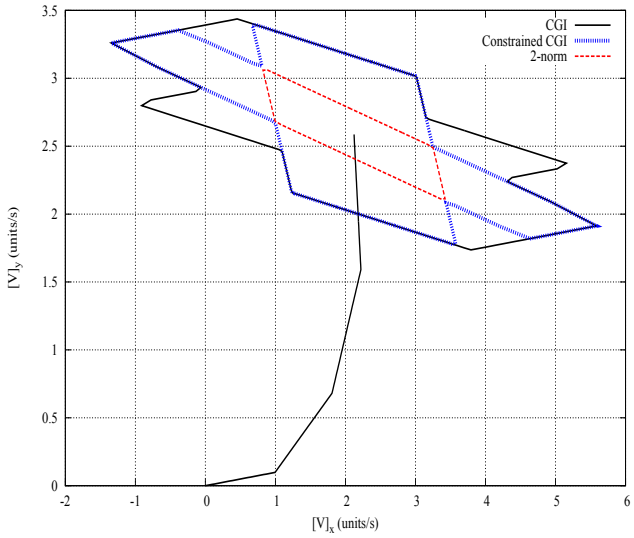

Figure 3.9: Maximum achievable end-effector velocities in configuration A using 2-norm, CGI, and constrained CGI resolution

Chapter 4

Extended Cascaded Generalized Inverse Resolution (eCGI)

In the previous chapter we introduced an alternative to 2-norm resolution and CGI resolution for systems in which continuity of resolution is a serious concern. However this cannot possibly represent all systems. CGI has been successfully implemented in a number of systems and not explicitly impeded their performance. Therefore for systems in which discontinuity in resolution is not an absolutely discriminating factor or for systems which have been sufficiently tested to ensure discontinuity does not arise, the additional output space of CGI resolution outweighs the certainty of continuity in cCGI resolution.

In the following chapter it will be demonstrated that, although it has until the work of this thesis been considered the largest extension of 2-norm, CGI still does not attain the full potential output range of arbitrary systems. An extension of CGI resolution, termed the Extended Cascaded Generalized Inverse, or eCGI is introduced and shown applied to resolved kinematic redundancy. This chapter contains the work of [C5].

4.1 Limits of resolution range of CGI

In the following example, we will show that despite successfully extending the resolution range of the 2-norm, CGI fails to extend resolution to the full potential output space of arbitrary systems. Again, the considered example is resolution of kinematic redundancy resolution, however this time in the acceleration domain. For the following example let Configuration B represent the following arm states:

Configuration B:
$\boldsymbol{q} = [\frac{\pi}{32}, \frac{\pi}{4}, \frac{\pi}{4}, \frac{\pi}{4}]$ (rad)
$\dot{\boldsymbol{q}}(t=0) = [0,0,0,0]$ (rad/sec)

$\boldsymbol{\tau}_{\max} = [5, 1, 1, 1]$ (Nm)

Consider an arm in configuration B. We are free to make $\tau_{1_{\max}}$ larger than the other motors, since motor 1 would be mounted on the base and therefore would not contribute to increased arm inertia. Coriolis and inertial forces are neglected as they will not affect the redundancy resolution. For simplicity, $\boldsymbol{M}$ will be considered as the identity matrix. The arm will be considered horizontally-planar, so gravity forces can also be neglected.

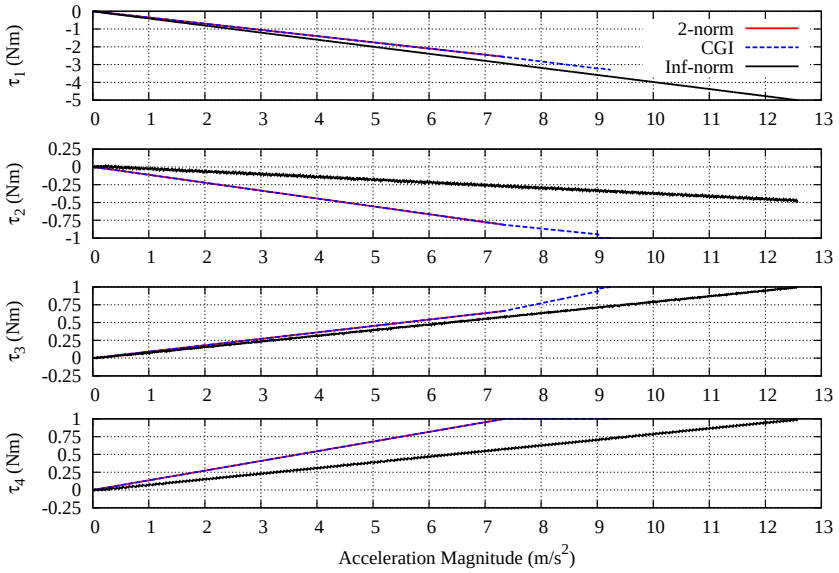

Figure 4.1: Resolution of joint torques for given acceleration magnitude using 2-norm, CGI, and infinity-norm resolution. CGI is seen to successfully extend the realizable output over 2-norm, but not to the level possible using infinity-norm resolution.

Fig. 4.1 illustrates a static resolution of the kinematic redundancy in this arm. For given acceleration magnitude in the direction of $\theta = 335$ degrees, the resolved joint torques using 2-norm, CGI, and infinity-norm resolution are shown. It is seen that the 2-norm is the first to fail at $\|a\| \approx 7$ (m/s^2), due to excess τ_4 task assignment. CGI on the other hand is able to extend the resolution range to $\|a\| \approx 9$ (m/s^2) by truncating 2-norm-saturated inputs and redistributing their output contributions. However, looking at the infinity-norm resultant we can see the system is capable of even greater output potential. Using infinity-norm resolution extends the feasible output of this system to over 12 (m/s^2), which is guaranteed by the definition of the infinity-norm to be the maximum system-capable acceleration.

Fig. 4.2 illustrates the maximum end-effector acceleration (scaled down by a factor of 10) possible in all directions in configuration B using 2-norm, CGI, and

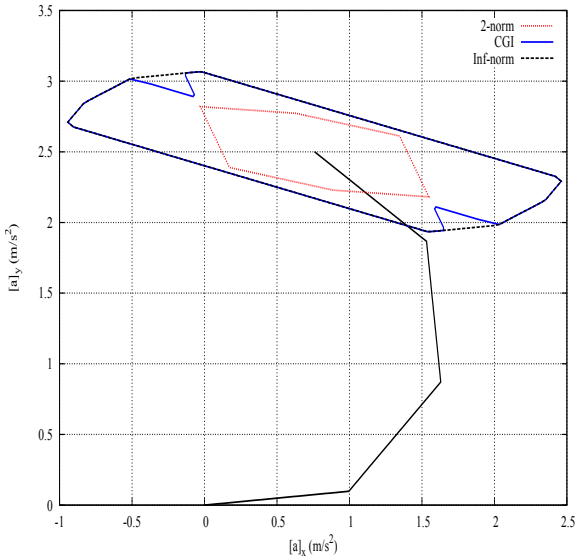

Figure 4.2: Scaled maximum end-effector acceleration achievable using 2-norm, CGI resolution, and infinity-norm resolution. CGI is seen to extend resolution range of 2-norm, but not to the full system capability represented by infinity-norm.

infinity-norm resolution. It is seen that although successful in extending the resolution range of 2-norm in all but a few trivial points, CGI still fails to extend the resolution of the system to the full system-capable output range. CGI additionally suffers from a lack of directional isotropy in the clipped output space regions, which might tempt further artificial reduction of the output space.

4.2 Proposal: Extended Cascaded Generalized Inverse Resolution (eCGI)

Figure 2.1 illustrates our proposed answer to this problem, the Extended Cascaded Generalized Inverse, or eCGI. eCGI is the current largest extension of 2-norm resolution.

The structure of eCGI parallels that seen in CGI. In CGI, the system is resolved using 2-norm; if the resolution fails the result is truncated and re-resolved using 2-norm. In eCGI, the system is resolved with CGI; if resolution using CGI fails, combinations of CGI-saturated inputs are de-saturated and the system is re-resolved using CGI.

The structure of eCGI takes advantage of the physical relationship between

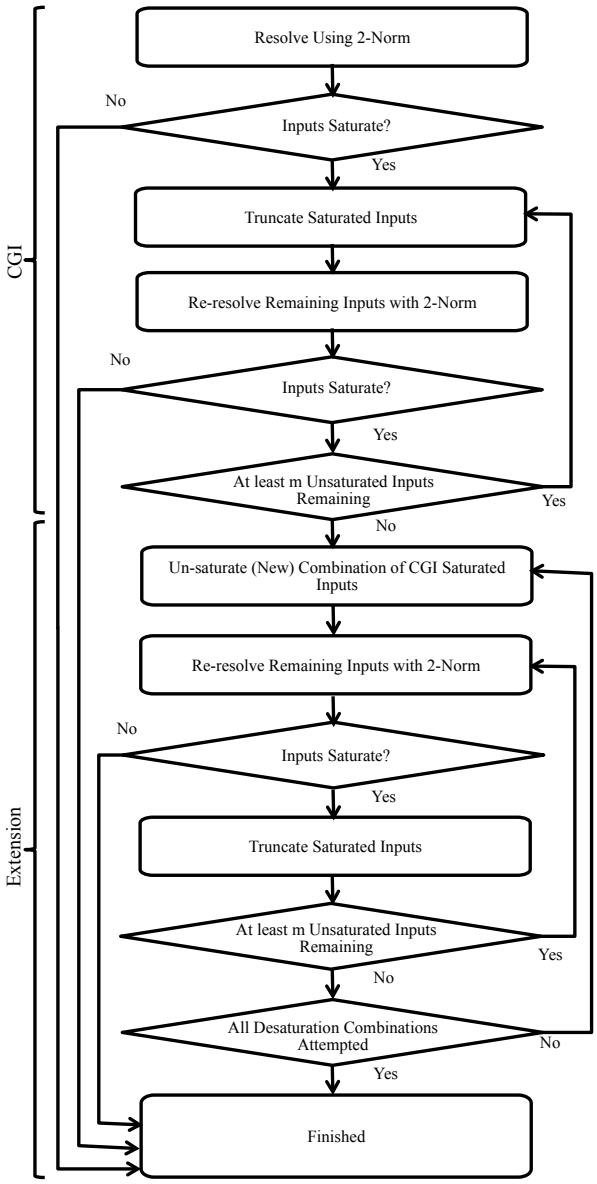

Figure 4.3: Flowchart of Extended Cascaded Generalized Inverse redundancy resolution.

2-norm and infinity-norm resolution. The problem of limited output space in CGI resolution can be rephrased as a problem of CGI saturating inputs inconsistently with those saturated by infinity-norm. This cannot be avoided, since the 2-norm and infinity-norm optimize along different criteria. However we can say that in

most physical systems the 2-norm and infinity-norm will often yield ”similar” results. As we have noted, a 2-norm optimization can be compared with a minimization of system energy, whereas an infinity-norm optimization is equivalent to a minimum effort resolution. It is physicall unlikely for a minimum-effort solution to be a particularly poor choice considering energy as a metric, and vice-versa. As such, typically when resolution is conducted using 2-norm and infinity-norm, the majority of saturated inputs will be shared. Those which saturate differently, due to unusual conflicts of effort versus energy will be the exceptions.

This effect can be observed in the previously conducted static resolution in Fig. 4.1. It can be seen that in resolution CGI and infinity-norm successfully saturates two of the three same inputs with the same sign. How to extend this example CGI resolution to the infinity-norm potential is simple: desaturating the ”incorrectly” saturated τ_2 and re-resolving the system subject to the ”correctly” saturated τ_1 and τ_3 will result in a continuous linear extension from the CGI failure point to the infinity-norm solution at the system-maximum output.

The generalization of this process results in our proposed eCGI.

4.3 Simulations and results

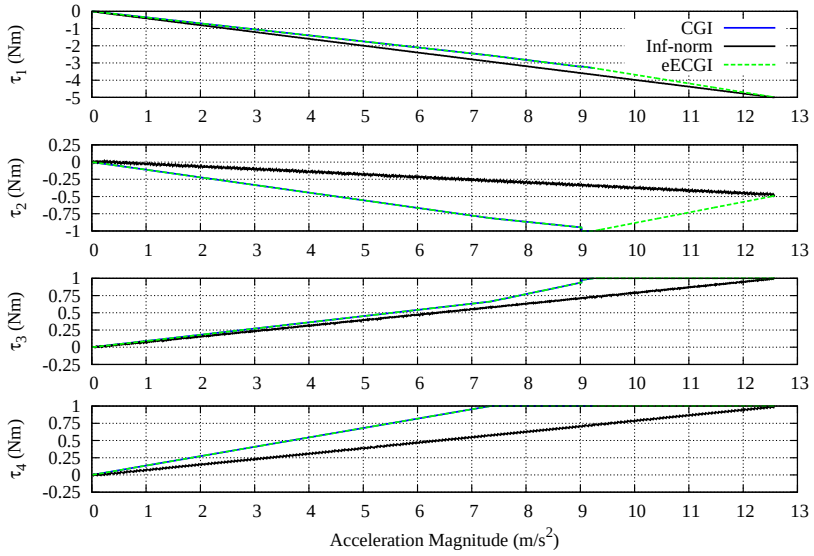

Figure 4.4: Resolution of joint torques for given acceleration magnitude using CGI, eCGI, and infinity-norm resolution. eCGI is seen to successfully extend the realizable output from CGI to the full system capability.

Fig. 4.4 illustrates the simulation shown in Fig. 4.1 repeated using CGI, eCGI, and infinity-norm resolution. CGI is seen to stop resolution at $\|a\| \approx 9$ (m/s^2) after saturating τ_4, τ_2, and τ_3, in that order. eCGI then successfully extends CGI resolution to infinity-norm resolution (both in acceleration magnitude and to the unique infinity-norm resolution at the system boundary) by desaturating τ_2 and re-resolving τ_2 and τ_1 subject to saturated τ_3 and τ_4.

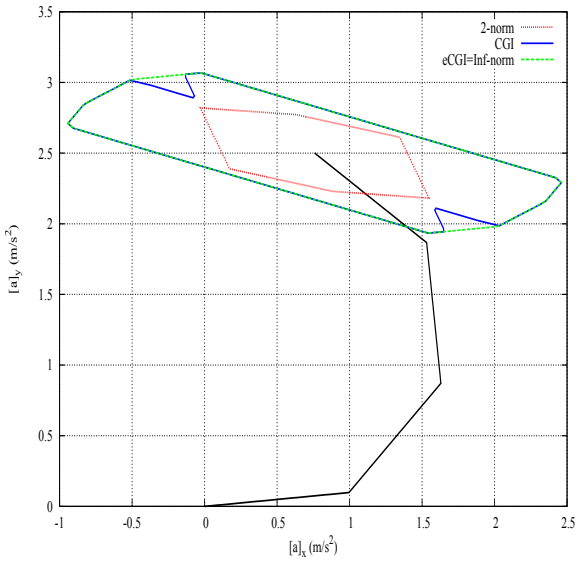

Figure 4.5: Scaled maximum end-effector acceleration achievable using 2-norm, CGI resolution, and eCGI resolution. Here, eCGI resolution can be seen extending the feasible output space to the full potential space.

Fig. 4.5 illustrates the simulation shown in Fig. 4.2 repeated using 2-norm, CGI, eCGI, and infinity-norm resolution. eCGI is seen to extend the maximum controllable end-effector acceleration from that possible with CGI to that possible with infinity-norm, which is by definition the maximum system capability.

4.4 Discussion

There are two drawbacks to eCGI resolution which should be emphasized. The first is the issue of discontinuity in eCGI resolution. As we have already seen, discontinuity exists in CGI resolution. Therefore eCGI, as an extension of CGI resolution also has the possibility for discontinuity in resolution. It should then be only applied after consideration has been made as to what effects may arise if discontinuity in resolution occurs, or if the system has been tested to ensure

discontinuity does not arise. If either of these are not feasible, then cCGI is the recommended resolution scheme, as it is the largest guaranteed continuous extension of the 2-norm.

The second issue in resolution is that there is no way, currently, of knowing a priori which combination of inputs ought to be de-saturated. Currently we can only recommend trying all possible combinations of inputs until one works. Some systemic way of determining which combination should be de-saturated would be a useful addition to the method. This issue however disappears in the case of single-degree redundant systems, which comprise a large portion of redundant systems. In a single-degree redundant system, there only exists a single option to de-saturate, significantly easing implementation and calculation time.

Chapter 5

2-norm/ Infinity-norm Switching Resolution of Biarticular Actuation Redundancy

In the previous two chapters, the methods were aimed at general systems and therefore the most important criteria is its simplicity in application to numerous systems.

If we restrict our consideration to a particular system, this opens the door for a more tailored approach and therefore greater utility. The considered system, biarticular actuation redundancy, is relatively simple but commonly utilized. These characteristics have allowed for the development of additional closed-form solutions for resolving redundancy, to supplement the commonly considered 2-norm solution. This has allowed us to propose 2-norm/Infinity-norm Switching Resolution of the redundancy in biarticularly actuated robot arms. The proposed method marks a first step at the long desired goal of bridging the 2-norm and infinity-norm resolution schemes.

Section 5.2 includes the work of [C3] and Section 5.3 includes the work of [C1].

5.1 Biarticular actuation

5.1.1 Overview

Fig. 5.1(a) illustrates a widely used model of the actuation in the human arm in 2-dimensions [40]. The arm is actuated by three pairs of antagonistic muscles. Muscle pairs e1 and f1 are monoarticular muscles which provide torque about the shoulder. Muscle pairs e2 and f2 provide torque about the elbow. The pairs

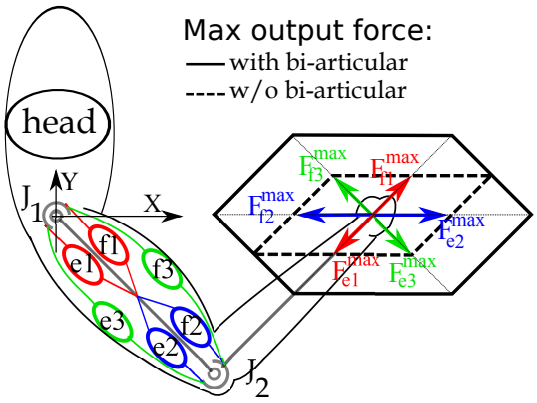

(a) At muscular level. Antagonistic muscle pairs co-contract to regulate torque and stiffness independently.

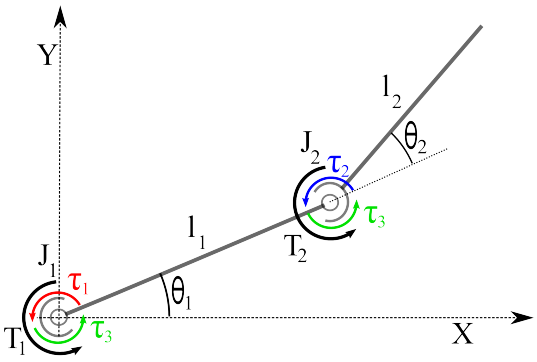

(b) Model of actuation using resultant torque of antagonistic muscles about joints 1 and 2 (J_1 and J_2).

Figure 5.1: Model of actuation in human arm [40]

e3 and f3 are biarticular muscles which provide torque about both the elbow and shoulder.

After collapsing antagonistic muscle pairs into their resultant torques, a simplified biarticular actuation model can be found in Fig. 5.1(b).

5.1.2 Resolution

The system in Fig. 5.1(b) is another particular case of (2.1) and can be represented by the following expression.

$$\begin{bmatrix} T_1 \\ T_2 \end{bmatrix} = \mathbf{B}\boldsymbol{\tau} = \begin{bmatrix} 1 & 0 & 1 \\ 0 & 1 & 1 \end{bmatrix} \begin{bmatrix} \tau_1 \\ \tau_2 \\ \tau_3 \end{bmatrix} \tag{5.1}$$

where T_1 and T_2 are output joint torques, τ_1 and τ_2 are the monoarticular actuator torques about joints 1 and 2 respectively, and τ_3 is the biarticular actuator torque actuating both joints.

Applying (2.4) allows computation of the 2-norm resolution of (5.1) as:

$$\tau_1 = \frac{2}{3}T_1 - \frac{1}{3}T_2 \tag{5.2}$$

$$\tau_2 = \frac{2}{3}T_2 - \frac{1}{3}T_1 \tag{5.3}$$

$$\tau_3 = \frac{1}{3}T_1 + \frac{1}{3}T_2 \tag{5.4}$$

Infinity-norm resolution of (5.1) can be expressed [40] by the following closed-form expression:

$$\tau_1 = \begin{cases} \frac{1}{2}(T_1 - T_2) & \text{if } T_1T_2 \leq 0 \\ T_1 - \frac{1}{2}T_2 & \text{if } T_1T_2 > 0 \text{ and } |T_1| \leq |T_2| \\ \frac{1}{2}T_1 & \text{if } T_1T_2 > 0 \text{ and } |T_1| > |T_2| \end{cases} \tag{5.5}$$

$$\tau_2 = \begin{cases} \frac{1}{2}(T_2 - T_1) & \text{if } T_1T_2 \leq 0 \\ \frac{1}{2}T_2 & \text{if } T_1T_2 > 0 \text{ and } |T_1| \leq |T_2| \\ T_2 - \frac{1}{2}T_1 & \text{if } T_1T_2 > 0 \text{ and } |T_1| > |T_2| \end{cases} \tag{5.6}$$

$$\tau_3 = \begin{cases} \frac{1}{2}(T_1 + T_2) & \text{if } T_1T_2 \leq 0 \\ \frac{1}{2}T_2 & \text{if } T_1T_2 > 0 \text{ and } |T_1| \leq |T_2| \\ \frac{1}{2}T_1 & \text{if } T_1T_2 > 0 \text{ and } |T_1| > |T_2| \end{cases} \tag{5.7}$$

Finally, application of CGI resolves (5.1) as

Case 0 :

$$\tau_1 = \tau_1^\dagger := \frac{2}{3}T_1 - \frac{1}{3}T_2 \tag{5.8}$$

$$\tau_2 = \tau_2^\dagger := \frac{2}{3}T_2 - \frac{1}{3}T_1 \tag{5.9}$$

$$\tau_3 = \tau_3^\dagger := \frac{1}{3}T_1 + \frac{1}{3}T_2 \tag{5.10}$$

Case τ_i(a) :

$$\tau_i = \tau_i^{\max} \tag{5.11}$$

$$\boldsymbol{\tau}_i' = (\mathbf{B}_i')^{-1}(\boldsymbol{T} - \mathbf{B}_i\tau_i^{\max}) \tag{5.12}$$

Case τ_i(b) :

$$\tau_i = -\tau_i^{\max} \tag{5.13}$$

$$\boldsymbol{\tau}_i' = (\mathbf{B}_i')^{-1}(\boldsymbol{T} + \mathbf{B}_i\tau_i^{\max}) \tag{5.14}$$

and define

$$\text{case 0 (2-norm)} := |\tau_i^\dagger| \leq \tau_i^{\max},\ i = 1,2,3 \tag{5.15}$$

$$\text{case } \tau_i\text{(a)} := \tau_i^\dagger > \tau_i^{\max},\ |\tau_i^\dagger| \geq |\tau_j^\dagger|,\ \forall j = 1,2,3 \neq i \tag{5.16}$$

$$\text{case } \tau_i\text{(b)} := \tau_i^\dagger < -\tau_i^{\max},\ |\tau_i^\dagger| \geq |\tau_j^\dagger|,\ \forall j = 1,2,3 \neq i \tag{5.17}$$

Where $\tau_i^{\max}$ is the maximum torque at motor i, $\boldsymbol{\tau}_i'$ is the vector $\boldsymbol{\tau}$ with the element τ_i removed, $\mathbf{B}_i$ is the i'th column of the matrix $\mathbf{B}$, and $\mathbf{B}_i'$ is the matrix $\mathbf{B}$ with the i'th column removed.

5.2 Proposal: 2-norm/Infinity-norm Switching Resolution

5.2.1 Concept

The connection of 2-norm and infinity-norm resolution has long been desired due to their opposing utility in different circumstances. That is, 2-norm is not an optimal resolution scheme for large output magnitudes, and the infinity-norm is not optimal for small output magnitudes. As we have seen, optimization using 2-norm

optimizes in analog to minimization of system energy. This is a reasonable optimization criteria for relatively small output magnitudes. However, we have also seen that when the output magnitude grows, the 2-norm has a tendency to request disproportionate exertion from individual inputs, even exceeding their limits. On the other hand, the infinity-norm minimizes the maximum exertion in the system. This is a very useful criteria for high output magnitudes, as it allows for the full benefit of the system's output space. However, when the desired output magnitude is low, of course the resolved inputs will be low and of little concern. Therefore infinity-norm resolution with a low output magnitude is effectively redundant.

Rather than using either method individually, it is clear then that a higher utility system would utilize 2-norm when the output magnitude is low and switch to infinity-norm when the output magnitude grows too large. Such a switching system was hypothesized by [41], but realization of such a switching system has met difficulty in implementation due to the lack of a closed-form solution of the infinity-norm. This has made speculation as to how to bridge the norms as well as analysis as to the continuity of the resultant system difficult. Instead compromises have been made in the form of 2-norm/infinity-norm weighted solutions in [42] and [43], but actual switching between the two remained unrealized. Thanks in great deal to the advent of a closed-form solution for infinity-norm resolution of biarticular resolution [40], we have succeeded in proposing the first realization of 2-norm/ infinity-norm switching resolution.

5.2.2 Proposal

A realization of the 2-norm/infinity-norm switching system for resolution of biarticular actuation redundancy has been proposed as follows:

$$\boldsymbol{\tau} = \begin{cases} \boldsymbol{\tau}^{\dagger}, & \text{if } |\tau_i^{\dagger}| \leq \tau_{\text{switch}},\ i = 1,2,3 \\ \boldsymbol{\tau}^{CGI}, & \text{if } \exists\, \tau_i^{\dagger},\ \text{s.t. } |\tau_i^{\dagger}| > \tau_{\text{switch}}, \\ & \text{and } |\tau^{CGI}| \leq \tau_{\text{switch}},\ i = 1,2,3 \\ \boldsymbol{\tau}^{\infty}, & \text{if } \exists\, \tau_i^{CGI},\ \text{s.t. } |\tau_i^{CGI}| > \tau_{\text{switch}} \end{cases} \tag{5.18}$$

where τ_{switch} is a selectable torque switching level used as $\tau_i^{\max}$ in the evaluation of CGI.

Proof of continuity of the proposed switching system can be found in Appendix B

A model of the proposed switching system can be seen in Fig. 5.2, which illustrates the utilized resolution scheme for a given desired output with unit τ_{switch}. This shape is characteristic of the switching system, with only the relative sizes of each section scaling with changing τ_{switch}.

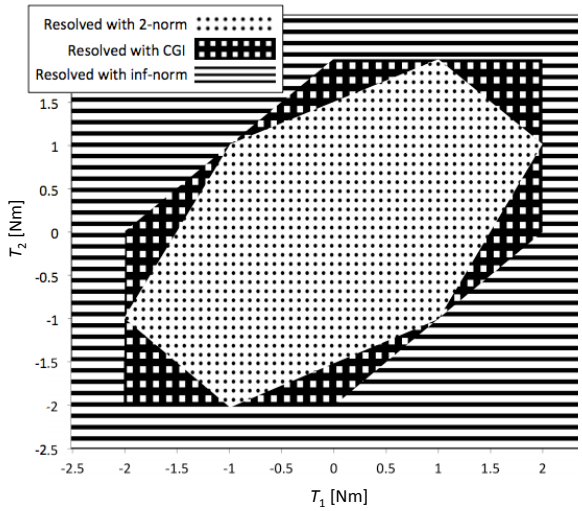

Figure 5.2: Visualization of proposed switching system with unit switching torque. The system resolves with respect to 2-norm until an infinity-norm threshold is met, at which point torques are reallocated and further optimized with respect to the infinity-norm.

Fig. 5.3 shows a view of the statics of the switching system. The graphs shows the resolved motor torques for given desired joint torques, in an arm described by (5.1). Resolution is carried out with unit τ_{switch}. The resulting waveform is a continuous function composed of three linear segments corresponding to 2-norm, CGI, and infinity-norm respectfully.

5.3 Experimental implementation

The following chapter describes an experimental implementation carried out testing the utility and veracity of our proposed switching resolution.

5.3.1 Setup

Hardware

For the purpose of testing our resolution system, a robotic arm with equivalent torque characteristics to Fig. 5.1(b) was developed. The arm can be seen in Fig. 5.4 and a schematic diagram of the developed arm can be seen in Fig. 5.5. The 2-link, planar arm is actuated by three motors. Motor 1 is fixed to the base and connected to a fixed pulley on joint 1, forming a monoarticular actuator on joint 1.

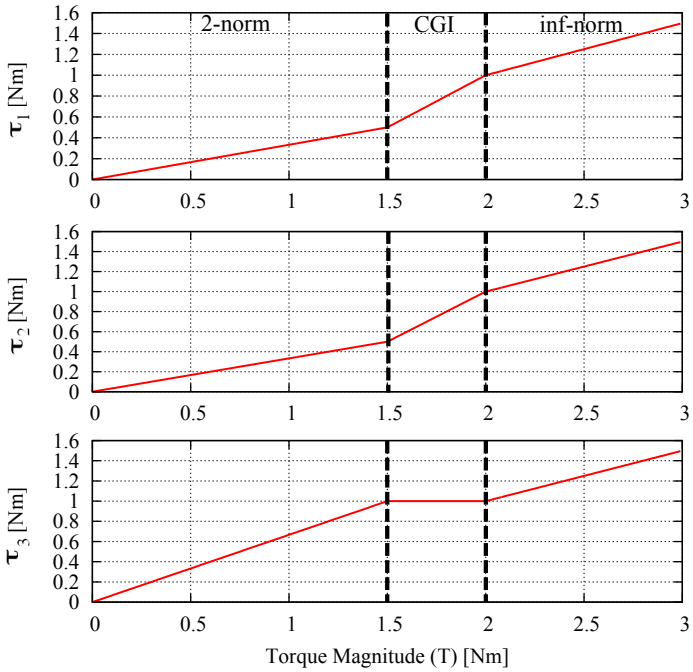

Figure 5.3: Simulation of switching system static torque resolution. The resultant waveform is a continuous function composed of three linear regions corresponding to 2-norm, CGI, and infinity-norm respectively.

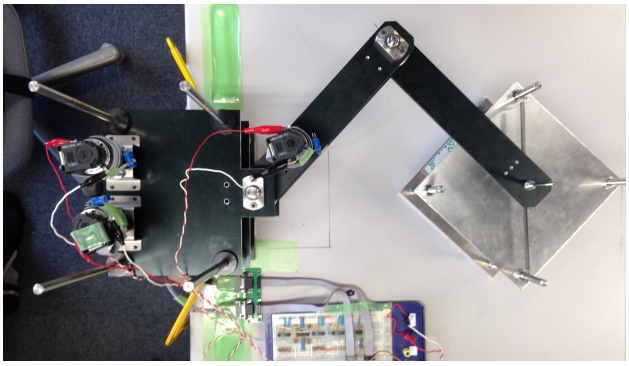

Figure 5.4: 2-link arm with two monoarticular actuators and one biarticular actuator connected to elastic resistance platform.

Motor 2 is fixed to link 1 and connected to a fixed pulley on joint 2, forming a monoarticular actuator on joint 2. Motor 3 is fixed to the base and is connected to a fixed pulley on joint 2 through a free pulley about joint 1, forming a biarticular actuator actuating both joints 1 and 2.

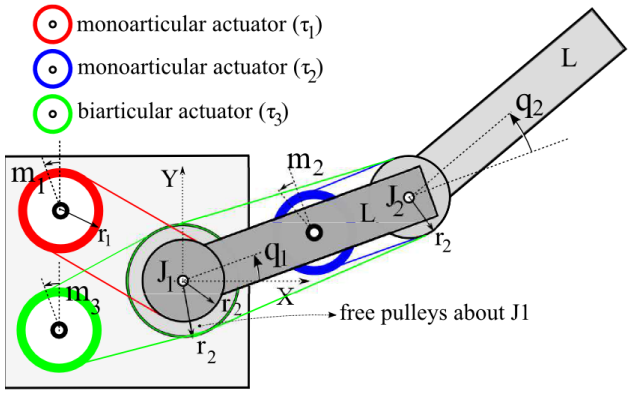

Figure 5.5: Schematic diagram of 2-link arm with two monoarticular actuators and one biarticular actuator utilized in experimental verification.

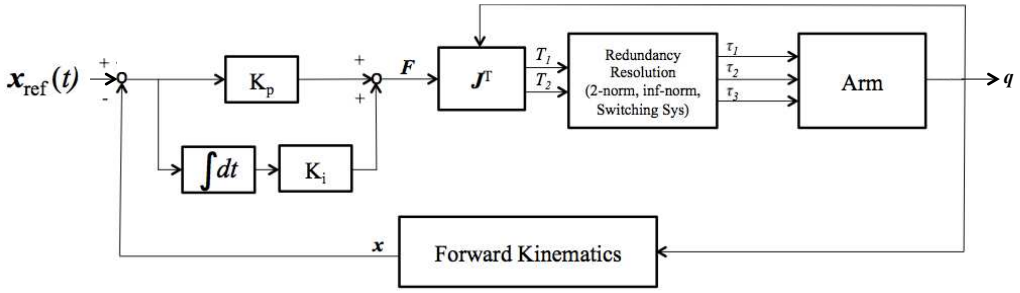

Figure 5.6: Block diagram of control strategy employed in experimental trials.

The arm is equipped with optical encoders about joints 1 and 2, enabling differential joint angle measurements. In order to compare electrical energy requirements, voltage probes are also placed on each motor.

The arm end-effector is affixed to an elastic resistance platform, which is composed of two steel square plates with four shafts connecting the two plates at each corner. The base plate is secured to the work bench. On two opposing shafts (in the positive and negative y direction for these experimental trials) two equivalent springs are connected to a shaft at the arm end-effector.

A list of relevant arm and elastic parameters can be found in Table 5.1.

Methodology

A block diagram of the control methodology utilized in the arm can be seen in Fig. 5.6. The end-effector position can be determined by the arm forward kinematics

Table 5.1: Arm parameters

Link Lengths (L)	0.25 m
Motor Model	Maxon DC Motor 148867
Motor Controller Model	Maxon Motor Controller ADS 50/5
Maximum Continuous Motor Torque	0.177 mNm
Motor Gain	30.2 mNm/A
Motor Pulley Inner Radius (r_1)	6 mm
Joint Pulley Inner Radius (r_2)	22.5 mm
Spring Coefficients	0.064 N/mm
Spring Natural Length	60 mm
Spring Prestretch Length	113 mm
Control Loop Frequency	833 Hz
Encoder Resolution	2000 Pls. (0.05 Degrees)
Voltage Measurement Resolution	5 mV

described by the following relationship.

$$\boldsymbol{x} = \begin{bmatrix} x \\ y \end{bmatrix} = \begin{bmatrix} \mathrm{L}\cos(q_1) + \mathrm{L}\cos(q_1 + q_2) \\ \mathrm{L}\sin(q_1) + \mathrm{L}\sin(q_1 + q_2) \end{bmatrix} \tag{5.19}$$

A PI controller was chosen as it lends itself to the simplest comparison of these three resolution schemes. We are only interested in the results of the redundancy resolution — particularly its continuity and the physical utility of the solution — so, as long as the task joint torque is equivalent across all three trials, the results are admissible. Task space proportional and integral gains are chosen empirically as $\mathrm{K_p} = 45$ N/m and $\mathrm{K_i} = 45$ N/(m $\cdot$ s).

The resultant force is translated to the joint space using the manipulator force-torque characteristics described by the following relationship:

$$\boldsymbol{T} = \boldsymbol{J}^T \boldsymbol{F} \tag{5.20}$$

With the desired joint torques calculated, the redundancy resolution is carried out using one of the redundancy resolution approaches (two-norm, infinity-norm, or switching resolution) and the motors are commanded with the resulting torques.

The test trajectory is assigned as follows. The arm begins at rest in a configuration of $\boldsymbol{q} = [\frac{\pi}{4}, -\frac{\pi}{2}]$ (rad), or $\boldsymbol{x} \approx [0.35, 0]$ (m). A cubic splines is constructed, taking the arm from its starting position to a desired position of $\boldsymbol{x} = [0.41, 0]$ (m) and back, taking 10 seconds in each direction. The direction of motion was chosen as it allows for the largest task-space displacement without risk of damaging the springs. The magnitude was chosen empirically so that the entire trajectory lies within the resolvable range of the maximum motor torques while 2-norm is used to resolve the redundancy. The time was chosen empirically to mitigate oscillation introduced by the elastic resistance platform.

When switching resolution is used to resolve system redundancy, the switching level τ_{switch} is assigned as 0.35 Nm, chosen empirically for this trajectory to best illustrate the difference between the three resolution methods.

5.4 Results

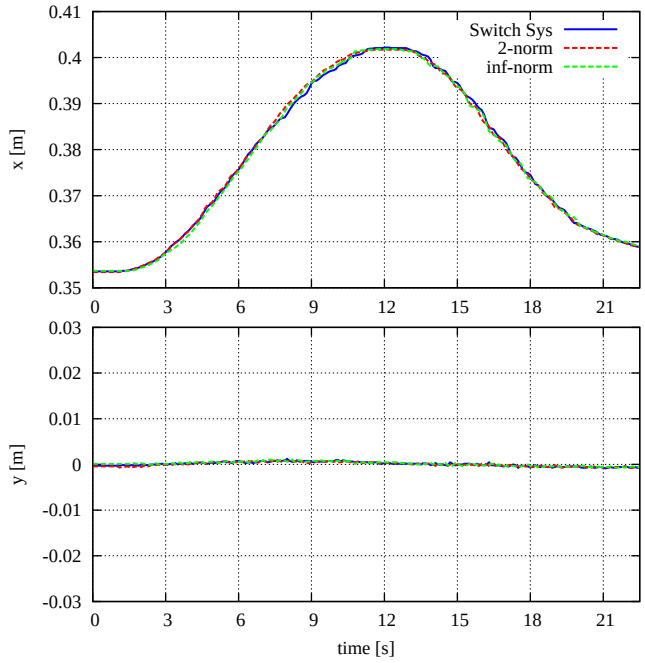

Figure 5.7: Task space position trajectories using 2-norm, infinity-norm, and switching resolution methods. The resolution method employed has no effect on the resultant trajectory as net joint torques are equivalent.

Fig. 5.7 illustrates the resultant end-effector position trajectories across time when 2-norm, infinity-norm, and switching resolution are employed in resolving

actuator redundancy. End-effector position is calculated by forward kinematics from recorded joint angles. As expected, the resultant position trajectories using each method are equivalent. This is to be expected as regardless of which redundancy resolution method is utilized, the resultant joint torques should still be the same. The redundancy resolution method varies only the levels of co-contraction, not the actual resultant torques. This is, however, a useful point of comparison. So long as the position trajectories of each trial are the same, we can neglect the effects of mechanical nonlinearities on our experimental results.

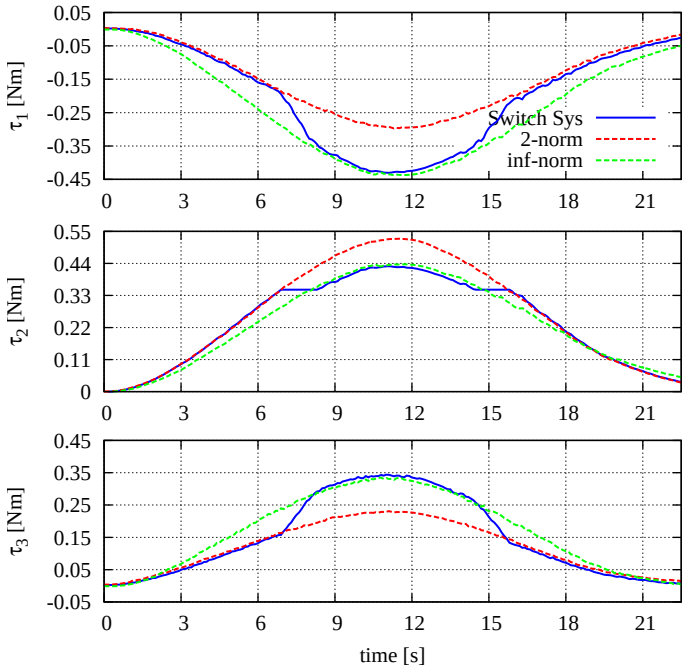

Figure 5.8: Resolved motor torques using 2-norm, infinity-norm, and switching resolution methods. The switching system is seen to switch continuously back and forth between 2-norm and infinity-norm at the defined switching level.

Fig. 5.8 illustrates the results of the redundancy resolution using each method. Until t=6.89 s both 2-norm and switching resolution resolve the system equivalently. At this point, the 2-norm resolved τ_2 exceeds τ_{switch} causing the switching system to switch to CGI resolution in order to reallocate motor torque. Switching resolution continues equivalent to CGI resolution until t=8.35 s, at which point reallocation completes and resolution switches to infinity-norm, conserving motor torque. Switching resolution is then equivalent to infinity-norm resolution until t=14.43 s, at which point the required output torque magnitude again allows for CGI resolution within input bounds. Finally resolution switches back to 2-norm

when possible at t=15.83 s. As asserted, the torques along the entire trajectory are resolved continuously.

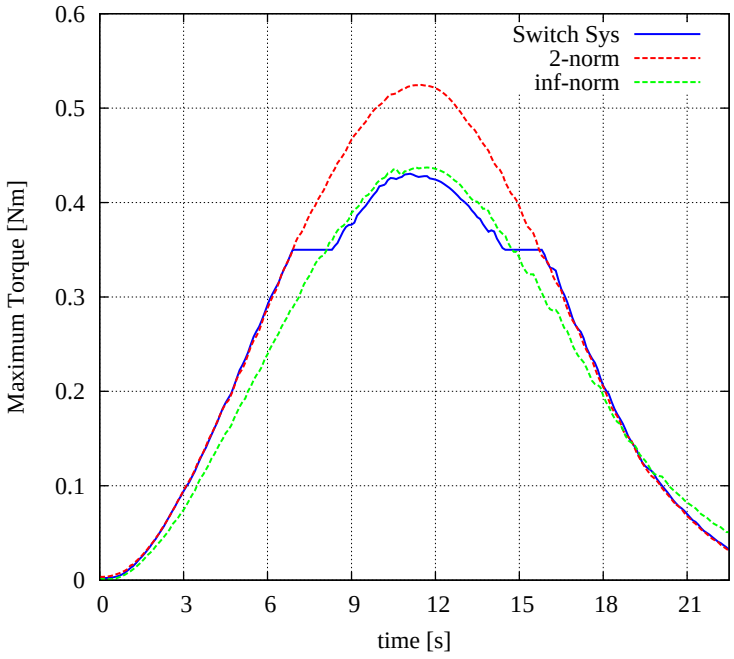

Figure 5.9: Maximum resolved motor torques using 2-norm, infinity-norm, and switching resolution methods. The switching system is seen to require equivalent maximum torque for this trajectory as the infinity-norm.

Fig. 5.9 illustrates the infinity-norm of the resolved motor torques (maximum resolved motor torque) of each resolution method over the entire trajectory of the arm. As anticipated while the requested torque magnitude is low, both 2-norm and switching resolution demand equal maximum motor exertion. When the maximum torque demanded by 2-norm exceeds the switching threshold of τ_{switch}, the maximum torque is held constant as torque is reallocated to τ_1 and τ_3. When reallocation completes, from t=8.35 to 14.43 s, infinity-norm and switching resolution demand equivalent maximum torque — this maximum torque is the minimal possible maximum torque given the desired output torque. Over the entire trajectory, 2-norm has a maximum required torque of 0.522 Nm. Switching resolution and infinity-norm resolution have a maximum torque requirement of 0.435 and 0.437 Nm, respectively. Therefore to accomplish the same trajectory 2-norm requires a motor with ≈ 20 percent larger torque capability than would be necessary for either switching or infinity-norm resolution.

Fig. 5.10 illustrates the input electrical energy over the arm trajectory. Mea-

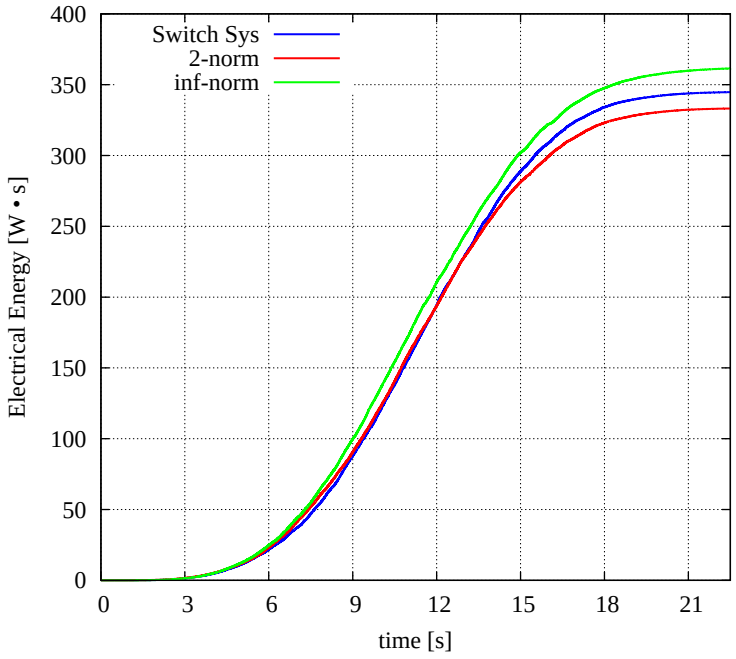

Figure 5.10: Electrical energy requirements using 2-norm, infinity-norm, and switching resolution methods. The switching system is seen to require equivalent power as 2-norm until the switching condition is met and maximum torque is prioritized.

sured voltages are filtered using a low pass Butterworth filter with f=0.2 Hz. The total input energy ($I.E$) is then measured the relationship:

$$I.E. = \int_0^t (V_1 I_1 + V_2 I_2 + V_3 I_3) dt \tag{5.21}$$

where V_i is the filtered motor voltage at motor i, and I_i is the current of motor I obtained by the command torque divided by the motor torque constant.

Since they resolve the system equivalently, it is found that 2-norm and switching resolution have equal energy demands until the two diverge at t=7.25 s. At t=7.25 s, switching resolution switches to CGI in order to sacrifice energy efficiency in order to prioritize safeguarding against overtaxing motors. After reallocation is complete, both infinity-norm and the switching system demand equivalent power from the system. The same relationship is seen again as switching resolution passes again through CGI and 2-norm resolution. Over the entire trajectory it is found that the infinity-norm requires 5 percent more electrical energy to realize the same trajectory as switching resolution. This difference in energy

Table 5.2: Relative comparison of performances of 2-norm, infinity-norm, and switching resolution across possible system configurations. Switching resolution is seen to perform preferably in all high priority criteria.

	Low Torque		High Torque	
	Electrical Energy (High Priority)	Maximum Torque (Low Priority)	Electrical Energy (Low Priority)	Maximum Torque (High Priority)
2-norm	Good	Bad	Best	Bad
Infinity-norm	Bad	Good	Worst	Good
Switching Sys.	Good	Bad	Middle	Good

can be attributed to infinity-norms greater degree of co-contraction during low-output magnitudes in order to ensure minimum system-wide exertion.

Table 5.2 compiles the results and compares the performance of 2-norm, infinity-norm, and the switching system across the possible system configurations observed. It is seen that the switching system uniquely performs preferably for all high priority criteria regardless of system configuration.

Chapter 6

Conclusions

In this thesis, a body of work on improving 2-norm based resolution methods for redundant systems was reviewed. In total, three methods were proposed targeting three different classes of redundant systems.

The first two methods — the Continuous Cascaded Generalized Inverse (cCGI) and the Extended Cascaded Generalized Inverse (eCGI) — are aimed at general systems in which the simplicity of 2-norm based resolution is a major benefit. The first of these, cCGI, is aimed at systems in which continuity of resolution is an absolute requirement. For these sorts of systems, cCGI is the largest extension of 2-norm which guarantees continuity. cCGI can therefore be applied to any system 2-norm is applied to without any significant dynamic affects, while improving the output space of the system. The second of these methods, eCGI, simply represents the largest extension of 2-norm resolution. In a numerical example in resolution of kinematic redundancy we showed eCGI was capable of extending the resolution to the full system capable output space. However like its predecessor, CGI, eCGI makes no guarantees of continuity in resolution.

These two methods, cCGI and eCGI form a binary approach at a wide selection of systems which have been dominated by 2-norm based resolution. Since all systems can be clearly distributed into continuity-vital and continuity-nonvital, we can easily determine which method is preferable for a particular system given the restriction. With little to no dynamic consequences cCGI can be applied to any system 2-norm can be applied to while allowing for a larger output space. If the dynamic consequences are negligible, eCGI can be applied for the largest extension of 2-norm based resolution.

The final method on the other hand, 2-norm/infinity-norm Switching Resolution, is proposed for a particular redundant system — biarticular actuation redundancy. This restriction of system renders the main benefit of 2-norm resolution (its simplicity) not so important. Several other methods have already been proposed in closed-form resolving this system. The presence of these methods however, al-

lowed us to propose the first realization of the long-desired 2-norm/infinity-norm switching resolution which allows for greater utility than using either alone in resolution. This resolution scheme was experimentally implemented in a robotic manipulator equipped with biarticular actuation redundancy, and was shown to reduce motor size requirements, with respect to 2-norm, while reducing electrical energy requirements, with respect to infinity-norm.

Points of possible future research additionally arise from the research presented in this thesis. Our proposal of 2-norm/infinity-norm switching resolution no doubt sheds light on a more general form for the system. We believe that eCGI combined with cCGI could provide for a more general implementation of the 2-norm/infinity-norm switching system or for a larger continuous extension of 2-norm resolution. Additionally a method to determine a priori suitable combinations of saturated inputs to de-saturate in eCGI would vastly improve implementation.

Appendix A

Proof of Continuity of cCGI Resolution

Here we will demonstrate continuity of the constrained Cascaded Generalized Inverse.

Let $\mathbf{B}$ be an mxn, full row rank matrix which translates actuation variables $\mathbf{u} \in \Re^n$ to task space values $\mathbf{v} \in \Re^m$ as in (2.1). Let $\mathbf{B}_i$, $\mathbf{B}'_{i_1.i_2...i_z}$, u_i, and $\mathbf{u}'_{i_1.i_2...i_z}$ be as originally defined in section 3.2. We will first demonstrate continuity within each individual case and then demonstrate continuity during switching of cases, proving full piece-wise continuity.

In case 0 (when all 2-norm satisfying inputs are within their respective maximum bounds), the solution is equivalent to the pseudoinverse solution. If $\mathbf{B}$ is full row rank, the solution is continuous within case 0 by the continuity property of the pseudoinverse.

In case $i_1(x_1).i_2(x_2)...i_{z-1}(x_{z-1}).i_z(\mathrm{a})$, the solution for $\mathbf{u}$ is of the form:

$$u_{i_1} = \begin{cases} u_{i_1 max} & \text{if } x_1 = \mathrm{a} \\ -u_{i_1 max} & \text{if } x_1 = \mathrm{b} \end{cases} \tag{A.1}$$

$$\vdots$$

$$u_{i_{z-1}} = \begin{cases} u_{i_{z-1} max} & \text{if } x_{z-1} = \mathrm{a} \\ -u_{i_{z-1} max} & \text{if } x_{z-1} = \mathrm{b} \end{cases} \tag{A.2}$$

$$u_{i_z} = u_{i_z max} \tag{A.3}$$

$$\mathbf{u}'_{i_1.i_2...i_z} = (\mathbf{B}'_{i_1...i_z})^{\dagger}(\mathbf{v} - \sum_{\gamma=1}^{z} \mathbf{B}_{i_\gamma} u_{i_\gamma}) \tag{A.4}$$

In this region, $u_{i_1}...u_{i_z}$ are constants which are clearly continuous, and $\mathbf{u}'_{i_1.i_2...i_z}$ may be rewritten as

$$\mathbf{u}'_{i_1.i_2...i_z} = (\mathbf{B}'_{i_1...i_z})^{\dagger}\mathbf{v} - (\mathbf{B}'_{i_1...i_z})^{\dagger}\sum_{\gamma=1}^{z}\mathbf{B}_{i\gamma}u_{i\gamma}) = (\mathbf{B}'_{i_1...i_z})^{\dagger}\mathbf{v} + \mathbf{k} \tag{A.5}$$

where $\mathbf{k}$ is a constant vector. If $\mathbf{B}'_{i_1...i_z}$ is full rank, $\mathbf{u}'_i$ is linear with respect to $\mathbf{v}$, by the continuity property of the pseudoinverse, and is therefore continuous.

A similar method shows continuity throughout case $i_1(x_1).i_2(x_2)...i_{z-1}(x_{z-1}).i_z(\mathrm{b})$.

Now that continuity has been demonstrated within each individual case, we now turn to demonstrating switching continuity.

While in case $i_1(x_1).i_2(x_2)...i_{z-1}(x_{z-1})$, the system is prompted to enter case $i_1(x_1).i_2(x_2)...i_{z-1}(x_{z-1}).i_z(\mathrm{a})$ when the value resolved in case $i_1(x_1).i_2(x_2)...i_{z-1}(x_{z-1})$ for input u_{i_z} becomes greater than $u_{i_z max}$. We must therefore demonstrate continuity at the condition:

$$\begin{aligned} &(\text{Case } i_1(x_1).i_2(x_2)...i_{z-1}(x_{z-1})), \\ &(u_{i_z}(i_1(x_1).i_2(x_2)...i_{z-1}(x_{z-1})) = u_{i_z max}), \\ \text{and } &(|u_{i_j}(i_1(x_1).i_2(x_2)...i_{z-1}(x_{z-1}))| \leq u_{i_j max}, \forall j \neq i) \end{aligned} \tag{A.6}$$

At this boundary, in case $i_1(x_1).i_2(x_2)...i_{z-1}(x_{z-1})$, removing the elements of $\mathbf{u}$ resolved as constants allows us to rewrite (2.1) as

$$\mathbf{v} = \sum_{\gamma=1}^{z}\mathbf{B}_{i\gamma}u_{i\gamma} + \mathbf{B}'_{i_1...i_z}\mathbf{u}'_{i_1...i_z} \tag{A.7}$$

$$\mathbf{B}'_{i_1...i_n}\mathbf{u}'_{i_1...i_z} = \mathbf{v} - \sum_{\gamma=1}^{z}\mathbf{B}_{i\gamma}u_{i\gamma} \tag{A.8}$$

It follows then that $\mathbf{u}'_{i_1...i_z}$ is the unique minimum 2-norm resultant for (A.8), else we could choose different elements for the vector $\mathbf{u}'_{i_1...i_{z-1}}(i_1(x_1).i_2(x_2)...i_{z-1}(x_{z-1}))$ corresponding to the elements of $\mathbf{u}'_{i_1...i_z}(i_1(x_1).i_2(x_2)...i_{z-1}(x_{z-1}))$ with the same or lower two norm while still resolving (2.1). But by definition, $\mathbf{u}'_{i_1...i_{z-1}}(i_1(x_1).i_2(x_2)...i_{z-1}(x_{z-1}$ is a minimum two norm solution for (2.1), so this is impossible by the uniqueness property of the pseudoinverse.

As such at the boundary condition, for case $i_1(x_1).i_2(x_2)...i_{z-1}(x_{z-1})$ we have:

$$\mathbf{u}'_{i_1...i_z} = (\mathbf{B}'_{i_1...i_z})^{\dagger}(\mathbf{v} - \sum_{\gamma=1}^{z}\mathbf{B}_{i\gamma}u_{i\gamma}) \tag{A.9}$$

Which is equal to the resolution of $\mathbf{u}'_{i_1...i_z}$ in case $i_1(x_1).i_2(x_2)...i_{z-1}(x_{z-1}).i_z(\mathrm{a})$. Since $u_{i_1}, u_{i_2}, \ldots, u_{i_z}$, and $\mathbf{u}'_{i_1...i_z}$ are resolved equivalently in case $i_1(x_1).i_2(x_2)...i_{z-1}(x_{z-1})$, and case $i_1(x_1).i_2(x_2)...i_{z-1}(x_{z-1}).i_z(\mathrm{a})$ at the switching condition, the system switches continuously between cases $i_1(x_1).i_2(x_2)...i_{z-1}(x_{z-1})$ and $i_1(x_1).i_2(x_2)...i_{z-1}(x_{z-1}).i_z($

A similar method demonstrates continuity between case $i_1(x_1).i_2(x_2)...i_{z-1}(x_{z-1})$ and $i_1(x_1).i_2(x_2)...i_{z-1}(x_{z-1}).i_z(\mathrm{b})$.

We will now demonstrate that, given the asserted constraint, that switching directly between any other cases is impossible. To do so, let us consider what would be required for such switching to actually occur. Suppose across k levels corresponding to u_{j_1} ... u_{j_k} a solution switches to another solution whose same levels now correspond to $u_{\tilde{j}_1}$ ... $u_{\tilde{j}_k}$, $u_{\tilde{j}_{\bar{k}}} \neq u_{j_{\bar{k}}}$, $\bar{k} = [1,k]$. Consider the lowest order of these switching occurrences, which correspond to variables u_{i_λ} and $u_{i_{\tilde{\lambda}}}$.

For a system to be in case $i_1(x_1).i_2(x_2)...i_{\lambda-1}(x_{\lambda-1}).i_\lambda(x_\lambda)$ the following must be satisfied:

$$|u_{i_\lambda}(i_1(x_1).i_2(x_2)...i_{\lambda-1}(x_{\lambda-1}))| > u_{i_\lambda max} \tag{A.10}$$
$$|u_{i_\Lambda}(i_1(x_1).i_2(x_2)...i_{\lambda-1}(x_{\lambda-1}))| \leq u_{i_\Lambda max},\ \forall \Lambda \neq \lambda \tag{A.11}$$

Likewise, for a system to be in case $i_1(x_1).i_2(x_2)...i_{\lambda-1}(x_{\lambda-1}).i_{\tilde{\lambda}}(x_{\tilde{\lambda}})$ the following must be satisfied:

$$|u_{i_{\tilde{\lambda}}}(i_1(x_1).i_2(x_2)...i_{\lambda-1}(x_{\lambda-1}))| > u_{i_{\tilde{\lambda}} max} \tag{A.12}$$
$$|u_{i_\Lambda}(i_1(x_1).i_2(x_2)...i_{\lambda-1}(x_{\lambda-1}))| \leq u_{i_\Lambda max},\ \forall \Lambda \neq \tilde{\lambda} \tag{A.13}$$

Thus, the only border case that exists between these two cases occurs when:

$$|u_{i_\lambda}(i_1(x_1).i_2(x_2)...i_{\lambda-1}(x_{\lambda-1}))| = u_{i_\lambda max} \tag{A.14}$$
$$|u_{i_{\tilde{\lambda}}}(i_1(x_1).i_2(x_2)...i_{\lambda-1}(x_{\lambda-1}))| = u_{i_{\tilde{\lambda}} max} \tag{A.15}$$
$$|u_{i_\Lambda}(i_1(x_1).i_2(x_2)...i_{\lambda-1}(x_{\lambda-1}))| \leq u_{i_\Lambda max},\ \forall \Lambda \neq \lambda, \tilde{\lambda} \tag{A.16}$$

which is in neither case $i_1(x_1).i_2(x_2)...i_{\lambda-1}(x_{\lambda-1}).i_\lambda(x_\lambda)$ nor $i_1(x_1).i_2(x_2)...i_{\lambda-1}(x_{\lambda-1}).i_{\tilde{\lambda}}(x$ Thus it is impossible to switch directly between cases $i_1(x_1).i_2(x_2)...i_{\lambda-1}(x_{\lambda-1}).i_\lambda(x_\lambda)$ and $i_1(x_1).i_2(x_2)...i_{\lambda-1}(x_{\lambda-1}).i_{\tilde{\lambda}}(x_{\tilde{\lambda}})$, due to the continuity property of the pseudoinverse. Due to the case conditions of the considered higher order switching case, it is also now evident that switching between these generalized two cases is impossible.

Finally we will show that, given the asserted constraints, that switching directly between a and b cases of the same level and variable is impossible. To do so, let us consider what would be required for such switching to actually occur. Suppose across k levels corresponding to u_{j_1} ... u_{j_k} a solution switches to another case where the corresponding a's and b's of these k variables invert. Consider the lowest order of these switching occurrences, which corresponds to variables u_{i_λ}.

For a system to be in case $i_1(x_1).i_2(x_2)...i_{\lambda-1}(x_{\lambda-1}).i_\lambda(\mathrm{a})$ the following must be satisfied:

$$u_{i_\lambda}(i_1(x_1).i_2(x_2)...i_{\lambda-1}(x_{\lambda-1})) > u_{i_\lambda max} \tag{A.17}$$

Likewise, for a system to be in case $i_1(x_1).i_2(x_2)...i_{\lambda-1}(x_{\lambda-1}).i_\lambda(\mathrm{b})$ the following must be satisfied:

$$u_{i_\lambda}(i_1(x_1).i_2(x_2)...i_{\lambda-1}(x_{\lambda-1})) < -u_{i_\lambda max} \tag{A.18}$$

No boundary points exist between these two cases, so by the continuity property of the pseudo-inverse, switching directly between these two cases is impossible. Due to the case conditions of the considered higher order switching case, it is also now evident that switching between these generalized two cases is impossible.

A similar method proves that direct case switching combining switches in level variables and switching of a and b cases of the same level variable are impossible, given the asserted constraints.

Appendix B

Proof of Continuity of 2-norm/Infinity-norm Switching Resolution

In this section, the continuity of the proposed switching system will be demonstrated. CGI is defined such that it is continuous with increased torque magnitude (maintaining the ratios of T_1 and T_2, and is clearly continuous while re-optimized with respect to a single saturated motor torque. If discontinuity were to arise within CGI, it would occur while switching the input to be saturated and re-optimized against. Such switching events occur when two 2-norm torque resolutions simultaneously saturate.

To demonstrate CGI's continuity over the entire domain, we will show that at these simultaneous saturation events that the resolution with respect to both variables is equivalent. Further we will show that at such conditions, the 2-norm resolution is equal to the infinity-norm resolution (so these saturated variables cannot be re-optimized against). Note, this section of proof will concern itself with desired outputs s.t. $T_1, T_2 \neq 0$. A desired output with T_1 or T_2 equal to zero is a specific case which will be analyzed separately as part of the next section.

With CGI demonstrated as continuous with the infinity-norm at simultaneous saturation events, sequential saturation events will then be considered. It will be demonstrated that after 2-norm saturates and the other torques are re-optimized, when a subsequent motor torque saturates, the resolution is equal to the infinity-norm solution.

B.0.1 At least one saturated variable of 2-norm/CGI must be shared in the solution of the inf-norm

Analysis of the closed-form solutions of the 2-norm, CGI, and infinity-norm yield the following possible forms of resolutions for nonzero output torques:

	τ_1	τ_2	τ_3
$T_1 > 0$ $T_2 > 0$	+	+	+
	+	−	+
	−	+	+
$T_1 > 0$ $T_2 < 0$	+	−	+
	+	−	−

A useful characteristic of the infinity-norm is that its solution always has two or more inputs resolved as equal to the maximum value of the resolution.

Likewise, CGI fails to resolve after two or more inputs saturate. Although from the information given alone, it cannot be said that at this point the CGI resolution is equal to the infinity-norm solution, it can be said that at least one of the saturated variables is shared by both solutions.

Therefore the following can be said. If multiple variables saturate in 2-norm resolution and re-optimization with respect to neither results in increased output potential, the 2-norm resolution at this point is equal to the infinity-norm resolution. If a single variable saturates in 2-norm, CGI is used to re-optimize, and further re-optimization with respect to the variable which saturates in CGI resolution does not yield further output potential, the CGI resolution is equal to the infinity-norm resolution at that point. If re-optimization after CGI is possible, the resolution at the highest torque magnitude in that direction is equal to the infinity-norm resolution.

The remaining sections of proof will demonstrate:

1. Re-optimization after 2 simultaneous saturations, and re-optimization after CGI resolution are further unnecessary.

2. 2-norm is equal to infinity-norm during simultaneous saturations, and that in subsequent saturation events, CGI resolution is equal to infinity-norm.

Note, only the cases $(T_1, T_2 > 0)$ and $(T_1 > 0, T_2 < 0)$ will be considered. $(T_1, T_2 < 0)$ and $(T_1 < 0, T_2 > 0)$ are duals of these two cases.

B.0.2 Continuity at equal saturation rates

$T_1, T_2 > 0$

$\tau_1, \tau_2, \tau_3 \geq 0$

- τ_1, τ_2 saturate simultaneously

$$\tau_1 = \frac{2}{3}T_1 - \frac{1}{3}T_2 = \tau^{\max} \tag{B.1}$$
$$\tau_2 = \frac{2}{3}T_2 - \frac{1}{3}T_1 = \tau^{\max} \tag{B.2}$$
$$\implies T_1 = T_2 \implies \tau_3 = 2\tau_1 = 2\tau^{\max} \tag{B.3}$$

  Which is a contradiction, so this condition cannot actually occur.

- τ_1, τ_3 saturate simultaneously

$$\tau_1, \tau_3 = \tau^{\max} \implies T_1 = 2\tau^{\max} \tag{B.4}$$

  Clearly T_1 can't be resolved higher than $2\tau^{\max}$, so here the 2-norm resolution is equal to the infinity-norm resolution.

- τ_2, τ_3 saturate simultaneously

  Dual of τ_1, τ_3 saturating simultaneously.

$\tau_1, \tau_3 \geq 0, \tau_2 \leq 0$

- τ_1, τ_2 saturate simultaneously

$$\tau_1 = \frac{2}{3}T_1 - \frac{1}{3}T_2 = \tau^{\max} \tag{B.5}$$
$$\tau_2 = \frac{2}{3}T_2 - \frac{1}{3}T_1 = -\tau^{\max} \tag{B.6}$$
$$\implies T_1 = -T_2 \tag{B.7}$$

  Which is a contradiction since both $T_1, T_2 > 0$, so this condition cannot actually occur.

- τ_1, τ_3 saturate simultaneously

  Dual of $\tau_1, \tau_2, \tau_3 \geq 0, \tau_1, \tau_3$ saturate simultaneously.

- τ_2, τ_3 saturate simultaneously

$$\tau_2 = -\tau^{\max}, \tau_3 = \tau^{\max} \tag{B.8}$$
$$\implies T_2 = 0 \tag{B.9}$$
$$\implies \tau_1 = \frac{2}{3}T_1 = 2\tau_3 = 2\tau^{\max} \tag{B.10}$$

  Which is a contradiction, so this condition cannot actually occur.

$\tau_2, \tau_3 \geq 0, \tau_1 \leq 0$ Dual of $\tau_1, \tau_3 \geq 0, \tau_2 \leq 0$

$T_1 > 0, T_2 < 0$

$\tau_1, \tau_3 \geq 0, \tau_2 \leq 0$

- τ_1, τ_2 saturate simultaneously

  We note that either maximum τ_1 or maximum τ_2 (or both) must exist in the infinity norm solution in this configuration. We assume τ_1 is maximum in the infinity norm solution, and that if τ_1 and τ_2 saturate at a torque magnitude of k (corresponding to $T_1(k)$ and $T_2(k)$) that there is some realizable output with a larger magnitude $k + \Delta k$ in the same direction (whose resolution linearly approaches the infinity norm solution at the maximum attainable torque). At this point we resolve the system is resolved as

$$\tau_1 = \tau^{\max} \tag{B.11}$$
$$\tau_3 = T_1(k) + \Delta k T_1(k) - \tau^{\max} \tag{B.12}$$
$$\tau_2 = T_2(k) + \Delta k T_2(k) - T_1(k) - \Delta k T_1(k) + \tau^{\max} \tag{B.13}$$
$$= -\tau^{\max} + \Delta k T_2(k) - \Delta k T_1(k) \tag{B.14}$$
$$\implies \tau_2 < -\tau^{\max} \tag{B.15}$$

  Which is a contradiction, so one cannot attain a higher magnitude output in the same direction with maximum τ_1. A similar process shows the same for τ_2. Therefore one cannot produce a higher magnitude torque in the same direction. This implies that the 2-norm solution is equal to the infinity norm solution at this point.

- τ_1, τ_3 saturate simultaneously

  Dual of $T_1, T_2, \tau_1, \tau_2, \tau_3 > 0$: τ_1, τ_3 saturate simultaneously.

- τ_2, τ_3 saturate simultaneously

$$\tau_2 = -\tau^{\max}, \tau_3 = \tau^{\max} \tag{B.16}$$
$$\implies T_2 = 0 \tag{B.17}$$

  Which is a contradiction, so this condition cannot actually occur.

$\tau_1 \geq 0, \tau_2, \tau_3 \leq 0$ Dual of $\tau_1, \tau_3 \geq 0, \tau_2 \leq 0$.

B.0.3 CGI equal to inf-norm at max. realizable torque

With the case of simultaneous saturation of 2-norm demonstrated to be equal to the infinity-norm, we will now demonstrate single input saturation in 2-norm, followed by saturation of another variable in CGI also yields an infinity-norm equivalent resolution. Let such notation as $\tau_1 \rightarrow \tau_2$ represent the condition that the left input saturates in 2-norm, the system is re-evaluated in CGI with respect to the left input, and the right input saturates in the CGI re-resolution.

$T_1, T_2 > 0$

$\tau_1, \tau_2, \tau_3 \geq 0$

- $\tau_1 \rightarrow \tau_2$

$$T_2 - (T_1 - \tau^{\max}) = \tau^{\max} \tag{B.18}$$
$$\implies T_1 = T_2 \tag{B.19}$$
$$\tag{B.20}$$

  Therefore τ_1 and τ_2 saturate at the same time. This case was covered in section B.0.2, and it was shown that it cannot actually occur.

- $\tau_2 \rightarrow \tau_1$

  Dual of $\tau_1 \rightarrow \tau_2$

- $\tau_1 \rightarrow \tau_3$, $\tau_2 \rightarrow \tau_3$, $\tau_3 \rightarrow \tau_1$, $\tau_3 \rightarrow \tau_2$

  Duals of $T_1, T_2, \tau_1, \tau_2, \tau_3 > 0$: Simultaneous saturation of τ_1 and τ_3.

$\tau_1, \tau_3 \geq 0, \tau_2 \leq 0$

- $\tau_1 \rightarrow \tau_2$

$$T_2 - (T_1 - \tau^{\max}) = -\tau^{\max} \tag{B.21}$$
$$\implies T_1 - T_2 = 2\tau^{\max} \tag{B.22}$$
$$T_1 \leq 2\tau^{\max} \implies \tau_2 \leq 0 \tag{B.23}$$

  Which is a contradiction, so this condition cannot actually occur.

- $\tau_2 \rightarrow \tau_1$

  Dual of $\tau_1 \rightarrow \tau_2$

- $\tau_1 \rightarrow \tau_3$

  Dual of $T_1, T_2, \tau_1, \tau_2, \tau_3 > 0$: Simultaneous saturation of τ_1 and τ_3.

- $\tau_2 \to \tau_3$

$$\tau_3 = T_2 + \tau^{\max} = \tau^{\max} \tag{B.24}$$
$$\implies T_2 = 0 \tag{B.25}$$

  Which is a contradiction. Therefore, this condition cannot occur.

- $\tau_3 \to \tau_2$
  Dual of $\tau_2 \to \tau_3$

$\tau_2, \tau_3 \geq 0, \tau_1 \leq 0$ Dual of $\tau_1, \tau_3 \geq 0, \tau_2 \leq 0$

$T_1 > 0, T_2 < 0$

$\tau_1, \tau_3 \geq 0, \tau_2 \leq 0$

- $\tau_1 \to \tau_2$, $\tau_2 \to \tau_1$
  Dual of $T_1 > 0$, $\tau_1, \tau_3 \geq 0$, $T_2 < 0$, $\tau_2 \leq 0$: τ_1 and τ_2 saturate simultaneously

- $\tau_1 \to \tau_3$, $\tau_3 \to \tau_1$
  Dual of $T_1, T_2 > 0$, $\tau_1, \tau_2, \tau_3 \geq 0$: Simultaneous saturation of τ_1 and τ_3.

- $\tau_2 \to \tau_3$, $\tau_3 \to \tau_2$
  Dual of $T_1, T_2 > 0$, $\tau_1, \tau_3 \geq 0$, $\tau_2 \leq 0$, $\tau_2 \to \tau_3$.

$\tau_2, \tau_3 \leq 0, \tau_1 \geq 0$ Dual of $\tau_1, \tau_3 \geq 0, \tau_2 \leq 0$

$T_1 > 0, T_2 = 0$

In this case, 2-norm resolves the system as

$$\tau_1 = \frac{2}{3} T_1 \tag{B.26}$$
$$\tau_2 = -\frac{1}{3} T_1 \tag{B.27}$$
$$\tau_3 = \frac{1}{3} T_1 \tag{B.28}$$

τ_1 will saturate at $T_1 = \frac{3}{2}\tau^{\max}$ and larger torques will be reevaluated by CGI as

$$\tau_1 = \tau^{\max} \tag{B.29}$$
$$\tau_2 = -(T_1 - \tau^{\max}) \tag{B.30}$$
$$\tau_3 = T_1 - \tau^{\max} \tag{B.31}$$

Both τ_2 and τ_3 will saturate when $T_1 = 2\tau^{\max}$. Since all three torques are saturated, this CGI resolution is equal to the infinity-norm solution at this point.

Other Cases

$(T_1 < 0, T_2 = 0), (T_1 = 0, T_2 > 0)$, and $(T_1 = 0, T_2 < 0)$ are duals of $(T_1 > 0, T_2 = 0)$.
$(T_1, T_2 = 0)$ is a trivial case.

Bibliography

[1] T. Asfour and R. Dillmann, "Human-like Motion of a Humanoid Robot Arm Based on a Closed-Form Solution of the Inverse Kinematics Problem," in IEEE/RSJ Int. Conf. on Intelligent Robots and Systems, 2003, pp. 1407-1412.

[2] A. A. Maciejewski and C. A. Klein, "Obstacle Avoidance for Kinematically Redundant Manipulators in Dynamically Varying Environments," in The Int. Journal of Robotics Research, vol. 4, no. 3, pp. 109-117, Sep., 1985

[3] T. F. Chan and R. V. Dubey, "A Weighted Least-Norm Solution Based Scheme for Avoiding Joint Limits for Redundant Joint Manipulators," in IEEE Trans. on Robotics and Automation, vol. 11, no. 2, pp. 286-292, Aug., 2002.

[4] M Grebenstein et al, "The DLR Hand Arm System," in IEEE Int. Conf. on Robotics and Automation, Shanghai, China, 2011, pp. 3175 - 3182 .

[5] A. Bajo, R. E. Goldman, L. Wang, D. Fowler, and Nabil Simaan, "Integration and Preliminary Evaluation of an Insertable Robotic Effectors Platform for Single Port Access Surgery," in IEEE Int. Conf. on Robotics and Automation, Saint Paul, MN, 2012, pp. 3381 - 3387 .

[6] J. Zhang, H. Yu, F. Gao, and H. Zhao, "Key Issues in Studying Parallel Manipulators," in Int. Conf. on Advanced Mechatronic Systems, Zhengzhou, China, 2011, pp. 234 - 244 .

[7] L.W. Tsai, "Robot Analysis: The Mechanics of Serial and Parallel Manipulators," New York, John Wiley and Sons Inc.,1999.

[8] C. Yang, Q. Huang, H. Jiang, O. O. Peter, and J. Han, "PD control with gravity compensation for hydraulic 6-dof parallel manipulator," in Mechanism and Machine Theory, vol. 45, no. 4, pp. 666 - 677, Apr., 2010.

[9] Y. Yun and Y. Li, "Modelling and Control Analysis of a 3-PUPU Dual Compliant Parallel Manipulator for Micro Positioning and Active Vibration Isolation," in Journal of Dynamic Systems, Measurement and Control, vol. 45, no. 4, pp. 666 - 677, Apr., 2010.

[10] Q. Liang, D. Zhang, Z. Chi, Q. Song, Y. Ge, and Y. Ge, "Six-DOF micro-manipulator based on compliant parallel mechanism with integrated force sensor," in Robotics and Computer-Integrated Manufacturing, vol. 134, no. 2, p. 021001, 2012.

[11] Ball State University, "Human Arm Muscles Diagram," [online] Available: `http://libx.bsu.edu/cdm/ref/collection/AnatMod/id/211`.

[12] M. Kumamoto, T. Oshima, and T. Yamamoto, "Control properties induced by the existence of antagonistic pairs of bi-articular muscles– Mechanical engineering modeling analyses ," in Human Movement Science, vol. 15, no. 5, pp. 611-634, Oct., 1994.

[13] S. Wolf and G. Hirzinger, "A New Variable Stiffness Design: Mathcing Requirements of the Next Robot Generation," in IEEE Int. Conf. on Robotics and Automation, Pasadena, CA., 2008, pp. 1741 - 1746.

[14] T. Klein and M. A. Lewis, "A Robot Leg Based on Mammalian Muscle Architecture," in IEEE Int. Conf. on Robotics and Biomimetics, Guilin, China, 2009, pp. 2521 - 2526.

[15] V. Salvucci, S. Oh, Y. Hori, and y. Kimura, "Disturbance Rejection Improvement in Non-Redundant Robot Arms using Biarticular Actuators," in IEEE Int. Symp. on Industrial Electronics, Gdansk, Poland, 2011, pp. 2159 - 2164.

[16] T. Tsuji, C. Momiki, S. Sakaino, "Stiffness control of a pneumatic rehabilitation robot for exercise therapy with multiple stages," in *IEEE/RSJ Int. Conf. on Intelligent Robots and Systems*, Tokyo, 2013, pp. 1480-1485.

[17] M. A. Lewis, M. R. Bunting, B. Salemi, and H. Hoffmann, "Toward ultra high speed locomotors: Design and test of a cheetah robot hind limb," in *IEEE Int. Conf. on Robotics and Automation*, Shanghai, 2011, pp. 1990-1996.

[18] K. Tadano, M. Akai, K. Kadota, and K. Kawashima, "Development of grip amplified glove using bi-articular mechanism with pneumatic artificial rubber muscle," in *IEEE Int. Conf. on Robotics and Automation*, Anchorage, AK, 2010, pp. 23632368.

[19] R. Niiyama, S. Nishikawa, and Y. Kuniyoshi, "Athlete robot with applied human muscle activation patterns for bipedal running," in *10th IEEE/RAS Int. Conf. on Humanoid Robots*, Nashville, TN, 2010, pp. 498503.

[20] M.A.M. Dzahir, T. Nobutomo, and S.I. Yamamoto, "Antagonistic mono- and bi-articular pneumatic muscle actuator control for gait training system using contraction model," in *Biosignals and Biorobotics Conf.*, Rio De Janerio, 2013, pp. 1-6.

[21] Klein CA, Huang CH. Review of pseudoinverse control for use with kinematically redundant manipulators. IEEE Trans Syst. Man Cybern. 1983;13.2:245-250.

[22] T. L. Boullion and P. L. Odell, *Generalized Inverse Matrices*. Wiley- Interscience, 1971.

[23] O. Khatib, "Dynamic control of manipulators in operational space," in *6th IFToMM Congr. on Theory of Machines and Mechanisms*, New Delhi, 1983, pp. 1123-1131.

[24] I-C. Shim and Y-S. Yoon, "Stabilized minimum infinity-norm torque solution for redundant manipulators," *Robotica*, vol. 16, no. 2, pp. 193-205, 1998.

[25] H. Ding and J. Wang, "Recurrent neural networks for minimum infinity-norm kinematic control of redundant manipulators," *IEEE Trans. Syst. Man and Cybern. A., Syst. Humans*, vol. 29, no. 3, pp. 269-276, 1999.

[26] A. S. Deo and I. D. Walker, "Minimum effort inverse kinematics for redundant manipulators," *IEEE Trans. Robot. Autom.*, vol. 13, no. 5, pp. 767-775, Oct. 1997.

[27] Y. Zhang, J. Wang, and Y. S. Xia, "A dual neural network for redundancy resolution of kinematically redundant manipulators subject to joint limits and joint velocity limits," *IEEE Trans. Neural Netw.*, vol.14, no. 3, pp. 658-667, May 2003.

[28] I.A. Gravagne and I.D. Walker, "On the structure of minimum effort solutions with application to kinematic redundancy resolution," *IEEE Trans. Robot. Autom.*, vol. 16, no. 6, pp. 855-863, 2000.

[29] J.A.M Petersen and M. Bodson, "Constrained quadratic programming techniques for control allocation," *IEEE Trans. Control Syst. Technol.*, vol.14, no.1, pp.91-98, Jan. 2006.

[30] J. C. Virnig and David S. Bodden. "Multivariable control allocation and control law conditioning when control effectors limit (STOVL aircraft)," in *AIAA Guidance, Navigation, and Control Conf.*, Scottsdale, AZ., 1994, pp. 572-582.

[31] K. A. Bordignon, "Constrained control allocation for systems with redundant control effectors," Ph.D. Dissertation, Aero. Eng., Virginia Poly. Inst. and State. Univ., Blacksburg, 1996.

[32] D. Enns, "Control allocation approaches," in *Guidance, Navigation, and Control Conf. and Exhibit*, Minneapolis, MN., 1998, pp. 98-108.

[33] R.E Beck."Application of control allocation methods to linear systems with four or more objectives," Ph. D. Dissertation, Aero. Eng., Virginia Poly. Inst. and State. Univ., Blacksburg, 2002.

[34] Y. Zhang, C. A. Rabbath, and C. Y. Su, "Reconfigurable control allocation applied to an aircraft benchmark model," in *American Control Conf.*, Seattle, WA., 2008, pp. 1052-1057.

[35] Y. Zhang, V.S. Suresh, B. Jiang, and D. Theilliol, "Reconfigurable control allocation against aircraft control effector failures," in *IEEE Int. Conf. on Control Applications*, Singapore, 2007, pp. 1997-1202.

[36] A. Marks, J.F. Whidborne, and I. Yamamoto, "Control allocation for fault tolerant control of a VTOL octorotor," in *UKACC Int. Conf. on Control*, Cardiff, Wales, 2012, pp. 357-362.

[37] V. P. Bui, H. Kawai, Y. B. Kim, and K. S. Leei, "A ship berthing system design with four tug boats," *J. of Mechanical Science and Technology*, vol. 25, no. 5, pp. 1257-1264. May 2011.

[38] X. Shi, Y. Wei, J. Ning, and M. Fu, "Constrained control allocation using Cascading Generalized Inverse for dynamic positioning of ships," in *Int. Conf. on Mechatronics and Automation*, Beijing, China, 2008, pp. 1636-1640.

[39] A. De Luca, R. Farina, P. Lucibello, "On the Control of Robots with Visco-Elastic Joints," in *Int. Conf. on Mechatronics and Automation*, Barcelona, Spain, 2005, pp. 4297 - 4302.

[40] V. Salvucci, Y. Kimura, O. Sehoon, and Y. Hori, "Force maximization of bi-articular actuated manipulators using infinity norm," *IEEE Trans. Mechatron.*, vol. 18, no. 3, pp. 1080-1089. Jun. 2013.

[41] I. Gravagne and I. D. Walker, "Properties of Minimum Infinity-Norm Optimization Applied to Kinematically Redundant Robots," in *IEEE/ASME Int. Conf. on Intelligent Robots and Systems*, B.C., 1998, pp. 152-160.

[42] D. Guo and Y. Zhang, "Different-level two-norm and infinity-norm minimization to remedy joint-torque instability/divergence for redundant robot manipulators," *Robotics and Autonomous Systems*, vol. 60, no. 6, pp. 874-888, 2012.

[43] Y. Zhang, B. Cai, J. Yin, and L. Zhang, "Two/infinity norm criteria resolution of manipulator redundancy at joint-acceleration level using primal-dual neural network," *Asian Journal of Control*, vol. 14, no. 4, pp. 1036-1046, 2012.

List of Publications

Journals

[C1] **T. Baratcart**, V. Salvucci, and T. Koseki, "Expermental Verification of Two-norm, Infinity-norm Continuous Switching Implemented in Resolution of Biarticular Actuation Redundancy," *Advanced Robotics*. [Submitted].

International Conference- First Author

[C2] **T. Baratcart**, V. Salvucci, and T. Koseki, "On the continuity of cascaded generalized inverse redundancy resolution, with application to kinematically redundant manipulators," in *IEEE Industrial Electronics Conf.*, Vienna, Austria, 2013.

[C3] **T. Baratcart**, V. Salvucci, and T. Koseki, "2-norm/infinity-norm continuous switching resolution in biarticularly actuated robot arms," in *The 13th Int. Workshop on Advanced Motion Control*, Yokohama, 2014.

[C4] **T. Baratcart**, V. Salvucci, and T. Koseki, "Dynamic Analysis of Continuous Cascaded Generalized Inverse Resolution of Kinematically Redundant Manipulators with Flexible Joints," in *The 13th European Control Conf.*, Strasbourg, France, 2014.

[C5] **T. Baratcart**, V. Salvucci, and T. Koseki, "Extending the Resolution Range of the Cascaded Generalized Inverse," in *The IEEE/ASME International Conf. on Advanced Intelligent Mechatronics*, Strasbourg, France, 2014.

International Conference- Second Author

[C6] V. Salvucci, **T. Baratcart**, and T. Koseki, "Increasing Isotropy of Intrinsic Compliance in Robot Arms through Biarticular Structure," in *19th World Congress of the International Federation of Automatic Control*, Cape Town, South Africa, 2014.

[C7] V. Salvucci, **T. Baratcart**, and T. Koseki, "Analytical Study on Increasing Isotropy of Intrinsic Stiffness in Manipulators through Biarticular Structure," in *The IEEE/ASME International Conf. on Advanced Intelligent Mechatronics*, Strasbourg, France, 2014.